LA-6626-MS
Formal Report

Special Distribution

Issued: December 1976

Feasibility of Detecting Artificial Magnetic Anomalies in Hydrofractured Rock by Superconducting Gradiometer-SQUID Systems

by

W. C. Overton, Jr.

los alamos
scientific laboratory
of the University of California
LOS ALAMOS, NEW MEXICO 87545

UNITED STATES
ENERGY RESEARCH AND DEVELOPMENT ADMINISTRATION
CONTRACT W-7405-ENG. 36

DISCLAIMER

FEASIBILITY OF DETECTING ARTIFICIAL MAGNETIC ANOMALIES IN HYDROFRACTURED ROCK BY SUPERCONDUCTING GRADIOMETER-SQUID SYSTEMS

by

W. C. Overton, Jr.

ABSTRACT

We have carried out a study of the signal physics of magnetic anomaly detection by superconducting gradiometer-SQUID systems to determine the feasibility of possible applications to the geothermal energy program. Such systems would make full use of the incredible sensitivity of the superconducting quantum interference device (SQUID) which can be in the range of 10^{-11} Oe in practical device applications. In addition to magnetic anomalies in the earth's field produced by spherical distributions of magnetic matter, we have also considered anomalies that would be artificially produced by flooding magnetic material into cracks produced by hydrofracturing in deep boreholes drilled into dry rock geothermal sources. The study indicates that surface detection by horizontal and vertical gradiometers of crack anomalies will not be feasible if the magnetic material flooding the crack is a paramagnetic solution. However, one can concoct a slurry to carry prepolarized ferromagnetic particles of a size sufficiently large to permit domain formation but small enough to permit rotation and alignment in the earth's field. In this case, the anomaly signal is large enough to permit extraction of anomaly orientation information out of the background of magnetic noise and earth's field gradients. The superconducting gradiometer-SQUID system is shown to be exceptional in its capability of removing undesirable magnetic noise and gradients. We find the greatest promise in systems that would be comprised of a magnetometer or gradiometer that could be lowered into the borehole to positions opposite the formations cracked by hydrofracturing. Even in this case, the use of a paramagnetic material to produce the artificial anomaly will not provide signals of sufficient amplitude to overcome the magnetic noise. However, the slurry containing only one per cent by volume of ferromagnetic particles will produce a crack anomaly that is easily detectable by magnetometer or by the superconducting gradiometer-SQUID system. The study shows that the orientation angle of a crack anomaly, measured with respect to magnetic north, can be determined by a rotatable magnetometer or gradiometer with respectable accuracy. However,

the magnetometer measurement will contain the possibility of a 180° ambiguity, while the gradiometer measurement eliminates the ambiguity and is at least twice as accurate. We find also that a system of two surface gradiometers can be used to determine the orientation of the crack anomaly if the ferromagnetic particle volume ratio in the slurry is about ten per cent. In all of this work we assume a borehole depth of one mile and a crack of 2.0-mm width and radius of 300 m. Several new ideas for the extraction of anomaly information out of magnetic background noise and the presence of earth's field components and their gradients are proposed.

TABLE OF CONTENTS

FIGURES

I. INTRODUCTION

The recent discovery of the superconducting quantum interference device (SQUID) makes possible the detection of extremely small changes in magnetic fields.[1-5] The state of the art at the present time is such that rf SQUIDs operating at 30 MHz can detect magnetic field changes of 10^{-10} GHz $^{-1/2}$, while rf biasing at 450 MHz improves this to about 10^{-11} GHz $^{-1/2}$.[6,7] The state of present research on microwave SQUIDs indicates the possibility of detection sensitivities in the 10^{-14} G range.[6] Superconducting devices operating simply as magnetometers require sensitivities of only about 10^{-8} GHz $^{-1/2}$ because magnetic noise amplitudes of 10^{-4} to 10^{-8} G occupy a broad frequency spectrum and cause interference.[8,9] However, the use of the SQUID in conjunction with the superconducting gradiometer comprises a combination that takes full advantage of the incredible sensitivity of the SQUID while at the same time eliminating most of the broad-spectrum magnetic noise.[9] This inherent noise eliminating capability stems from the fact that the gradiometer measures the derivative of a magnetic field component, rather than the field value itself. Thus, terrestrial and celestial noise dipole and multipole sources contribute very small gradiometer noise signals because the fall off is $\sim 1/r^5$ and/or $1/r^7$.

A particular superconducting gradiometer-SQUID system is shown schematically in Fig. 1. The SQUID itself can be in the form of a tiny loop of superconducting Nb deposited on a rod or substrate. Typical loop inductances are of the order of 1 nH. Various methods of preparation of the weak link in this tiny loop, which comprises a Josephson junction, together with its normal metal shunt needed to achieve desired behavior and temperature characteristics, are very specialized but are now in fairly advanced stages of development and improvement.[10]

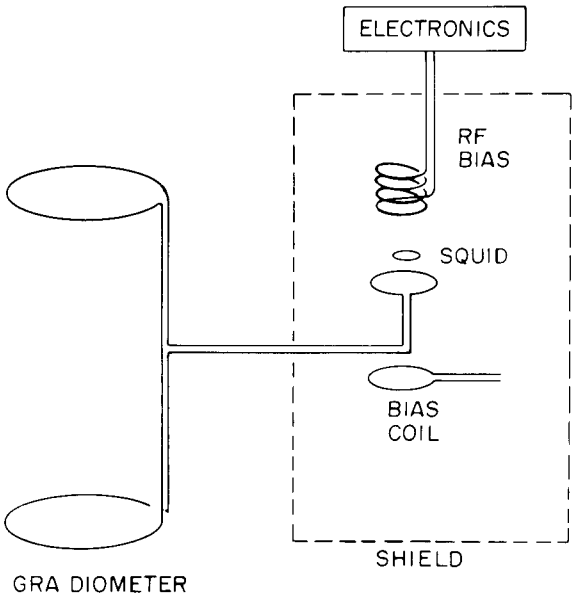

Fig. 1.
Schematic of superconducting gradiometer-SQUID system. All parts shown, except the electronics, are at liquid helium temperatures. Gradiometer loops have common axis (vertical in this configuration) and loop areas must be equal to parts in 10^5 to 10^7 and alignment to common axis to better than 10^{-4} radians. Adjustment tricks for equating loop response are not shown. The dashed area represents a superconducting shield. Weak link (not shown) in the SQUID inductor loop (inductance of order of 1 nH) has critical current in the microamp range.

Three or four commercial companies staffed by low temperature physicists manufacture SQUIDs and gradiometer-SQUID systems for military uses[11] while groups at NBS (Boulder, CO) and elsewhere are improving the development of gradiometer-SQUID systems for medical purposes.[12] The magnetocardiograms of human patients obtained by these devices show the same structure as conventional electrocardiograms, plus additional new features, without the need for electrodes in physical contact with the patient.[12] Research and development and demonstration in the area of detection and discovery of magnetic anomalies in the earth's field are being pursued in a number of laboratories.[13] There is considerable interest in the detection of magnetic anomalies produced by submarines. Each special application requires the development of its own particular gradiometer configuration and SQUID, as well as its own data acquisition and analysis system.

The purpose of this report is to investigate the feasibility of the application of gradiometer-SQUID systems to the LASL geothermal energy program. This program involves the drilling of boreholes into dry rock geothermal zones, the application of high pressures to borehole fluids to produce hydrofracturing of the rock zones, location of the splits, cracks and fissures produced by the hydrofracturing, and drilling a second hole to intersect this structure.[14] In practical use, water pumped down one borehole would flow through these cracks to the second borehole, become heated by the hot rocks in the process, and emerge as steam to run a power plant.[14] It is thus important to know in advance the orientation of the cracks produced by hydrofracturing so that the second borehole can be drilled in the correct location. One idea for detecting this orientation

emerged in a recent discussion between R. B. Duffield, LASL Q-Division Leader and W. E. Keller, LASL Q-26 Group Leader. This involved pumping magnetic material into the borehole from whence it flows into the hydrofractured structure. The earth's field would then polarize this material thereby producing a localized magnetic anomaly. The question was then whether or not the magnetic anomaly could be measured with sufficient accuracy to determine the orientation of the crack produced by hydrofracturing.

Because of the experience of the present author in the field of the signal physics of magnetic anomaly detection by superconducting gradiometer-SQUID systems,[9] he was asked to look into the feasibility of the above idea. The feasibility study is the subject of this present report. It is herein proven that a logging system designed to carry a certain superconducting gradiometer-SQUID configuration could determine the orientation of the hydrofractured crack, provided the material forced into the crack exhibits a sufficiently large magnetic moment per unit volume. Known paramagnetic materials in saturation solution are found not to have a sufficiently large susceptibility. However, prepolarized ferromagnetic particles in dilute suspension appear to satisfy the requirements of the problem. It is also found that the conventional flux gate sensor, operated in a magnetometer mode, can be used to detect the existence of the crack anomaly, but the determination of the crack orientation carries with it the possibility of an ambiguity of 180°. There appears to be no obvious trick for resolving this magnetometer ambiguity.

We also examine in this study the capabilities of surface magnetometers and of horizontal and vertical gradiometers for detecting the anomalies produced by hydrofracture cracks as well as by spherical distributions of magnetic material.

In Sec. II we apply the well-known formulas describing the earth's field at the geographic location of a nearby geothermal prospect, and calculate the magnetic moments this field produces in paramagnetic substances. We also examine the moments that would result from distributions of prepolarized ferromagnetic particles.

In Sec. III we study the fields at the surface that are produced by deep distributions of magnetic material polarized by the earth's field. We find the appropriate expressions for spherical distributions as well as for the so-called "wedge" distribution. The latter is chosen because of the convenience of integrating expressions in spherical coordinates and because the wedge distribution with a very small wedge angle $\Delta\phi$ closely approximates the case of a magnetic material pumped into the thin crack produced by hydrofracture.

In Sec. IV we obtain expressions describing signals that will be obtained by both magnetometers and superconducting gradiometers located in the borehole opposite formations cracked by hydrofracturing. In Sec. V we examine these expressions in order to compare the magnitudes of anomaly component, the earth's field gradient, the influence of magnetic noise, and the effects of imperfect construction of gradiometers.

In Sec. VI, we analyze the signals that will be produced by spherical and crack distributions at points on the surface and study the relative magnitudes of these signals in comparison with the earth's field gradient components, magnetic noise, and imperfection effects. The signals produced by an actual crack distribution is compared with that produced by a wedge used to approximate the crack distribution.

In Sec. VII, we give a summary and discussion of the results of the study and indicate several ways for overcoming the dominating and undesirable signal components that would otherwise prevent extracting the information contained in the anomaly signal. As an example, in some of the tricks proposed, we would operate two nearly identical rotating magnetometers or gradiometers in synchronism but otherwise at different locations. Subtraction or balancing these signals then eliminates much of the dominant but undesirable signal components. Such tricks could make feasible some otherwise unacceptable ideas.

II. MAGNETIC POLARIZATION BY THE EARTH'S FIELD

A. The Field Direction and Components

The magnetic material pumped into the fissures, cracks, and voids in the rocks surrounding the bottom of the borehole will become polarized by the earth's field. The direction of the magnetization vector (magnetic moment direction) should coincide with that of the local earth's field vector. In case the magnetic material is composed of solid particles of a ferromagnetic substance, the earth's field magnitude of about 0.5 gauss will be very small compared with the internal spontaneous magnetization field of the particles. Nevertheless, as discussed below in Sec. II-C, this small earth's field should align the large magnetization field because of the presence of thermal interactions. In the case of paramagnetic substances in solution, the local paramagnetic moment will always be parallel to the earth's field vector.

The earth's field horizontal and vertical components, H_h and H_r, respectively, can be calculated approximately for any set of geographical coordinates by

use of well-known formulas[15] for a dipole located at the earth's center, e.g.,

$$\begin{aligned} H_h &= H_o(a/r_a)^3 \sin\theta_e , \\ H_r &= 2H_o(a/r_a)^3 \cos\theta_e , \\ H_o &= 0.3035 , \\ a &= 6.371 \times 10^8 \text{ cm } (6371.2 \text{ km}). \end{aligned} \tag{1}$$

where a is the reference radius for a spherical earth and r_a is the actual radius of the point in question (bottom of borehole and geographical location). We will here assume $r_a = a$ because we are primarily interested only in field changes. The angle θ_e, which is defined as the geomagnetic colatitude, can be calculated via the formula [15]

$$\cos\theta_e = \cos\mu \cos\mu_o + \sin\mu \sin\mu_o \cos(\lambda - \lambda_o), \tag{2}$$

where μ is the geographic colatitude, $\mu_o = 11.44°$ is the geographic colatitude of the magnetic N-pole, and $\lambda_o = 290.24°$ is the east longitude of the N-pole.

We are presently interested in the earth's field at a location in the Jemez Mountains of New Mexico in the general vicinity of the geothermal sources near the Valle Grande. We arbitrarily pick the set of geographical coordinates 35°55'N; 106°30'W which corresponds to colatitude 54.083° and east longitude 253.5°. Substituting in Eq. (2) we obtain $\theta_e = 45.27°$ and

$$\begin{aligned} H_h &= 0.2199 \text{ Oe}, \\ H_r &= 0.4356 \text{ Oe}, \\ |\underset{\sim}{H}| &= 0.4880 \text{ Oe}. \end{aligned} \tag{3}$$

The direction of H_h is the same as that of the isogonic line for the above geographical coordinates which is about 13.7° E of true north. The field $\underset{\sim}{H}$ in Eq. (3) polarizes any localized magnetic material producing a vector moment

$$\underset{\sim}{m} = \underset{\sim}{i}\, m_x + \underset{\sim}{j}\, m_y + \underset{\sim}{k}\, m_z, \tag{4}$$

such that unit vector $\underset{\sim}{i}$ is parallel to the isogonic line and in the plane parallel to the earth's surface, $\underset{\sim}{j}$ is in this plane, and $\underset{\sim}{k}$ is perpendicular to it (vertical). The vector $\underset{\sim}{m}$ is shown schematically in Fig. 2.

Using this convention, we define the angle ψ according to

$$\begin{aligned} \sin\psi &= m_x/|m| = H_h/|H| = 0.45068\ldots , \\ \cos\psi &= m_z/|m| = H_r/|H| = 0.89268\ldots , \\ m_y &= 0 . \end{aligned} \tag{5}$$

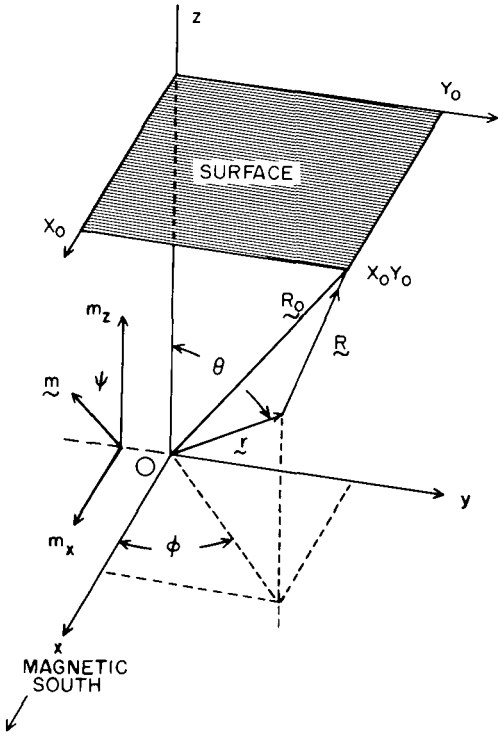

Fig. 2.
Spherical coordinate system for calculating anomaly contributions at any point such as X_o, Y_o on the surface. A volume element Δv_o at tip of vector r contains magnetic material, is polarized by the earth's field, and exhibits moment || to $\underset{\sim}{m}$. Origin 0 is at depth D of borehole below surface.

We show in Fig. 2 the induced magnetic moment vector $\underset{\sim}{m}$ pointing upward toward magnetic south rather than downward toward magnetic north. In applications of gradiometry it is unimportant whether we choose $\underset{\sim}{m}$ upward or $-\underset{\sim}{m}$ downward since the two sensing loops of the superconducting gradiometer are always connected in opposition. However, there is no difficulty in deducing the conventional direction of $\underset{\sim}{m}$.

The values of H_h, H_r in Eq. (3) could be in error as much as 10 per cent because of the presence of local moments not accounted for by the average formula Eq. (1). Such sources give rise to the so-called irregular part of the earth's field. In addition there is an external part due to magnetic sources outside the earth's atmosphere. There are also diurnal fluctuations of amplitudes as large as 100 γ (one $\gamma = 10^{-5}$ gauss). While a conventional or superconducting magnetometer sees the various fluctuations of the earth's field, the superconducting gradiometer

essentially screens them out, especially if the source is far away. Therefore, for our purposes, we shall not be concerned with the irregular part and the fluctuations and will be content to use the results in Eq. (3) to illustrate the principles of this paper. However, we shall give a more thorough discussion of the influence of noise on the gradiometer signal in Section V.

B. Paramagnetics in Solution

The paramagnetics of immediate interest are certain simple compounds that are highly soluble in water and exhibit, in the solution state, electron spin angular momenta in the range 1/2 $\hbar$ to 7/2 $\hbar$ per magnetic ion. The paramagnetic atoms with the largest total angular momenta are Fe, Ni, and Co and the rare earths Gd, Tb, Dy, Ho, Er, Tm, Cr.[16] Only Fe, Ni, and Co are feasible for present use because it would be too expensive to make up solutions with large amounts of rare earth atoms (hundreds to thousands of kg might be needed for some floodings). The experimentally determined "effective" magnetic moment per atom of Fe, in a high-temperature paramagnetic state, is actually larger than that of either Ni or Co. Moreover, bulk quantities of Fe compounds are considerably cheaper than those of Ni and Co. Therefore, we will confine our subsequent discussions to the most reasonable and practical materials, e.g., the various soluble Fe compounds.

One finds in the Handbook of Chemistry and Physics[17] a list of the solubilities of the various Fe compounds expressed in terms of the number of grams that will go into solution in 100 milliliters of water at room temperature and in hot water (they do not state the temperature of the hot water). It is easy to calculate from these data the number N of paramagnetic atoms per cm^3 in hot water. Since the temperature of present interest will be > 400 K, we expect to be able to dissolve much more paramagnetic material in the very hot solution than in the "hot" water of the tables. However, we shall here use the conservative figure of the tables.

We consider two Fe compounds, e.g., $FeCl_2$ (molecular wt 91.3) and $FeCl_3 \cdot 6H_2O$ (molecular wt 270), which have hot water solubilities of 106 g /100 cm^3 and 536 g /100 cm^3, respectively. These data then lead to the estimates of 0.012 $N_o Fe^{++}$ atoms/cm^3 (FeCl) and 0.02 $N_o Fe^{+++}$ atoms/cm^3 ($FeCl_3$), where N_o = Avogadro's number and $^{++}$ and $^{+++}$ represent divalent and trivalent states, respectively. There is not much point in considering Co and Ni compounds and other Fe compounds at this time because their solubilities are, according to the Handbook tables, less than those above.

The magnetic moment per unit volume of a paramagnetic substance is given, in the high-temperature approximation, by[16]

$$M = N\, g^2\, J(J+1)\, \mu_B^2\, H/3kT, \tag{6}$$

where N = number of paramagnetic atoms/cm^3, g = Landé g factor, J = L+S = total angular momentum, μ_B = Bohr magneton (0.927×10^{-20} erg/Oersted), H = applied field in Oersted, k = Boltzmann constant, and T = absolute temperature. It is convenient to rewrite the above formula in the form

$$M = N\, \mu_{eff}^2\, H/3kT\ , \tag{7}$$

in which we can use actual experimental values for the effective magnetic moment per atom (Note: this formula agrees with the older classical result due to Langevin and is valid only at high temperatures). The effective moment per atom is given by $\mu_{eff} = g[J(J+1)]^{1/2}\, \mu_B = n_{eff}\, \mu_B$, where n_{eff} is the effective number of Bohr magnetons per atom. Results for n_{eff} are to be found at a number of places in the literature. Kittel[16] summarizes the results for Fe ions as follows:

TABLE 1

EFFECTIVE MAGNETIC MOMENTS OF FERROUS IONS

Ion	Config-uration	Basic Level	$g[J(J+1)]^{1/2}$	n_{eff}(exptl)	g(exptl)
Fe^{++}	$3d^6$	$^5D_4$	6.7	5.4	2.2
Fe^{+++}	$3d^5$	$^6S_{5/2}$	5.92	5.9	2.0

Using now the solubilities given earlier in this section, the earth's field from **Eq.** (3), n_{eff} from the above table, and the formula Eq. (7), we obtain the magnetic moment per cm^3 of solution induced by the earth's field, as follows:

TABLE 2

MAGNETIC MOMENTS OF FERROUS PARAMAGNETICS IN SOLUTION

T (K)	$m_o(Fe^{++}$ in $FeCl_2)$	$m_o(Fe^{+++}$ in $FeCl_3)$
400	5.3×10^{-5}	10.61×10^{-5}
500	4.27×10^{-5}	8.49×10^{-5}
600	3.56×10^{-5}	7.07×10^{-5}

When a paramagnetic solution is flooded into a borehole which has been previously subjected to hydrofracture, the solution will then fill the fissures, cracks, and voids produced by the hydrofracturing. Since the total volume of these fissures, cracks, and voids is only a small fraction of the average rock volume of the surrounding region, the effective moment observed at some distance away will be greatly reduced. However, we can represent this reduction by use of a suitable "filling" factor denoted f_h. We will estimate f_h to be in the range 10^{-3} to 10^{-6}, depending on the effectiveness of the hydrofracturing process. We define f_h for a uniformly hydrofractured spherical region of effective radius at the end of the next section and for certain specific filled zones other than spheres in later chapters. For some volume element Δv located in a hydrofractured region of factor f_h, the effective moment observed at a distance can be expressed by

$$\Delta v \; f_h \; m_o(T). \tag{8}$$

C. Ferromagnetics in Slurry

We assume that it is possible to concoct a slurry with the following physical and chemical characteristics: (1) It can be pumped into the borehole under high pressures; (2) It can be forced into the cracks, fissures, and voids produced by previous hydrofracturing of a localized region of rocks surrounding the bottom of the borehole; (3) It shall be capable of carrying something like 1 to 10 per cent by volume of particles of some ferromagnetic substance; (4) The slurry must not react chemically with the particles, i.e., it must not dissolve them. Another requirement is that the magnetic "powder" or iron filings must be of sufficient size so as to exhibit true ferromagnetic behavior.

Assuming that the above requirements can be satisfied in practice, it should be possible to arrive at a reasonably accurate estimate of the ferromagnetic moment exhibited by unit volume of the slurry. However, certain aspects pertaining to the relationship between particle size, particle shape, and the direction of spontaneous magnetization in the particle must be discussed. If the magnetization directions of the many particles in a small volume element should tend to be random, then the net dipole field at some distance from the volume element would be zero. There are two distinct ways in which the earth's field can "align" the particle magnetization parallel to the earth's field direction. In the case of a nearly spherical Fe particle, the internal magnetization will not have any particular tendency to align with respect to a set of axes fixed to the particle (for example, the crystallographic axes) if the temperature is high. Therefore, the earth's field, even though only about 1/3000 of the particle internal field, in conjunction with the large thermal energy reservoir of the surrounding material, should tend to align the spontaneous magnetization vector. In case the particles have an elongated shape (e.g., iron filings) the internal magnetization has a tendency to align parallel to the long axis of the particle. The earth's field then exerts a weak force that can align the particle only if the viscosity of the slurry is small enough to permit rotation. When all of the elementary magnetization vectors are aligned parallel to the earth's field, then the material will exhibit the maximum magnetic moment. While this maximum probably cannot be achieved in practice, we expect the net moment can be a large fraction (perhaps 70% to 80%) of maximum by proper design of the slurry and choice of particles.

The list of ferromagnetic materials that can be produced in the form of small particles and satisfy, at the same time, the requirement of a high Curie-Weiss temperature, T_c, is essentially limited to iron and a few iron compounds. Only materials with $T_c > 700$ K are considered here to be acceptable and the list of possibilities includes metallic Fe, Fe_3Al, Fe_2B, Fe_3Cr, Fe_3P, FePt, Fe_3Si, and Fe_3Sn, of which only Fe_3Cr and FePt appear to be uneconomical. Some of these compounds appear to be ideal from the point of view of chemical binding energy, e.g., Fe_2B and Fe_3Si, in that they are unlikely to be soluble by the typical fluids that would be used in the slurry.

However, for purposes of magnetic field calculations discussed in later sections of this paper, we shall consider only solid Fe particles. The Curie-Weiss temperature for solid Fe is 1043 K and the spontaneous magnetization, M_o, at 0 K is 1760 $0e/cm^3$. For any $T < T_c$ the spontaneous (saturation) magnetization M_s

varies between M_o at 0 K and zero at T_c as shown by Fig. 3. Consider, for geothermal purposes, a temperature between 400 K and 600 K, and note, e.g., in Fig. 3 that M_s (600 K) is still 0.9 M_o. Thus, solid Fe particles should be ideal for use in the geothermal experiments proposed in Sec. I.

In one of the proposed practical methods, we would measure the magnetic field and field gradient changes at various points on the surface of the earth that are located a distance d away from the borehole, where d < about 1/2 D and D = depth of the borehole. Each volume element Δv of slurry forced into the cracks produced by hydrofracturing will contribute its own dipolar magnetic field. The dipole moment, which is proportional to the internal magnetization of all the particles in Δv, has the form

$$\Delta v \; f_s \; M_s(T), \tag{9}$$

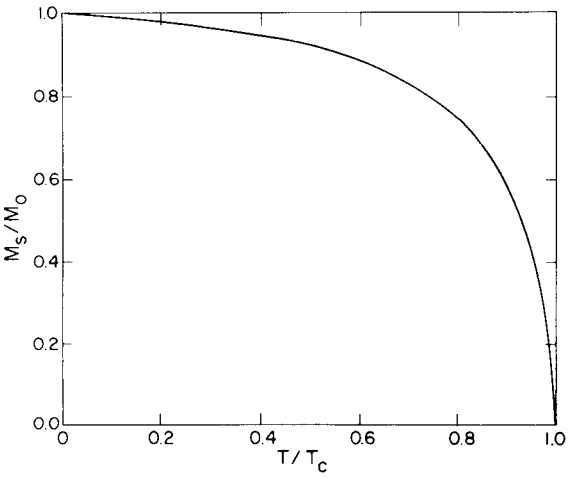

Fig. 3.
Saturation magnetization of ferromagnetic solid material as a function of temperature. Particles of sufficient size (greater than 10 to 100 μm) should retain remanent magnetism of 50 to 70 per cent of M_s when polarized in saturation field which is then reduced to zero. Refer to stopping point on typical hysteresis curve. Fe particles hold promise for use in dilute ferromagnetic slurry since T_c of 1043 K exceeds temperature of many geothermal sources.

where f_s = slurry filling factor = volume of magnetic particles per unit volume of slurry, and M_s is determined from the graph of Fig. 3.

When the hydrofracturing produces a more or less uniform (spherical) distribution of cracks around the bottom of the borehole there is the additional filling factor that must be taken into account. Let this be given by f_h = (volume of cracks filled with slurry)/(average spherical volume of region). The latter volume is just $4\pi\rho^3/3$, where ρ = average radius of hydrofractured region. It is desirable that the quantity f_h be as large as 10^{-3} but values as low as 10^{-6} must be expected. The effective dipole moment for such an idealized spherical region is then

$$\Delta v \; f_h \; f_s \; M_S(T) \; . \tag{10}$$

In practice, the magnetic material could be magnetized at the surface just prior to pumping the slurry into the borehole. This could be accomplished by flowing the slurry through a solenoidal magnet. If the particles have not been previously magnetized, their initial magnetization will follow the so-called virgin curve portion of the hysteresis curve. Assuming the field at the magnet center is large enough to produce magnetic saturation as the particles pass through, their magnetization will follow the standard hysteresis curve. As they flow out of the magnet to the point where the field is zero, they will then retain the remanent magnetization corresponding to 0.5 to 0.6 times the saturation value. However, as they now move into the high-temperature region, they will lose a certain amount of this remanent magnetization. The loss can be estimated from the curve of Fig. 3 if the temperature at the bottom of the borehole is known.

III. FIELDS AT THE SURFACE DUE TO DEEP DIPOLE SOURCES

A. The Basic Equations

The equations defining the magnetic fields due to a dipole source are well known. One can express the field $\underset{\sim}{B}(\underset{\sim}{R})$ due to a dipole at the origin of $\underset{\sim}{R}$ in terms of a parallel component $\underset{\sim}{e}_R B_{||}(\underset{\sim}{R})$, in which unit vector $\underset{\sim}{e}_R$ is $|| \underset{\sim}{R}$, and a perpendicular component $\underset{\sim}{e}_{\perp} B_{\perp}(\underset{\sim}{R})$, where $\underset{\sim}{e}_{\perp}$ is in the plane common to the magnetic moment vector $\underset{\sim}{m}$ and vector $\underset{\sim}{R}$ but $\perp$ to $\underset{\sim}{R}$. The geometry appropriate to the problem at hand is indicated in Fig. 2 which shows a right-handed coordinate system with origin 0 at the bottom of the borehole, with the x-direction parallel to magnetic south, the y-direction parallel to magnetic east, and the z-direction vertical. The surface of the earth is at constant z = D (D = depth of borehole). Let the magnetic material pumped into the borehole migrate to a point $\underset{\sim}{r}$ in the vicinity of 0 and exhibit a vector moment $\underset{\sim}{m} = \underset{\sim}{i}\, m_x + \underset{\sim}{k}\, m_z$, with $m_y = 0$; $\underset{\sim}{m}$ is parallel to the earth's field direction and makes the angle ψ with respect to z, as defined in Eq. (5).

A unit volume located at the tip of vector $\underset{\sim}{r}$ will contribute to the magnetic field on the surface an amount proportional to $\delta v |\underset{\sim}{m}| = \delta v\, m_o$, where $\delta v\, m_o$ is equivalent to (8) for a paramagnetic material or (10) for a ferromagnetic slurry. The point X_o, Y_o at which we require the field and field gradients is at a vector $\underset{\sim}{R}$ from the tip of $\underset{\sim}{r}$ and a vector $\underset{\sim}{R}_o$ from the origin 0. Let $\delta\underset{\sim}{B}$ be the contribution at X_o, Y_o due to $\delta v\, m_o$ at $\underset{\sim}{r}$. The components are given by

$$\delta\underset{\sim}{B}_{||} = \frac{2\underset{\sim}{R}(\underset{\sim}{R}\cdot\delta v\underset{\sim}{m})}{R^5}\ , \tag{11}$$

$$\delta\underset{\sim}{B}_{\perp} = \frac{\underset{\sim}{R}\ X\ \underset{\sim}{R}\ X\ (\delta v\underset{\sim}{m})}{R^5}\ , \tag{12}$$

$$\begin{aligned} R &= [(X_o-x)^2 + (Y_o-y)^2 + (D-z)^2]^{1/2} \\ &= [R_o^2 + r^2 - 2X_o x - 2Y_o y - 2Dz]^{1/2}. \end{aligned} \tag{13}$$

Note that $\underset{\sim}{m}$ and m_o are in units of magnetization (magnetic moment) per unit volume, i.e., the units are 0e, the same as the magnetic field ΔB.

The individual x-, y-, and z-components of $\delta\underset{\sim}{B}_{||}$ can be obtained by expanding the expression Eq. (11) and using $m_x = m_o \sin\psi$, $m_z = m_o \cos\psi$, $m_y = 0$. One finds

$$\delta B_{||}^{(x)} = 2\delta v\ m_o\ [(X_o-x)^2\sin\psi + (X_o-x)(D-z)\cos\psi]/R^5, \tag{14}$$

$$\delta B_{||}^{(y)} = 2\delta v\ m_o\ [(X_o-x)(Y_o-y)\sin\psi + (Y_o-y)(D-z)\cos\psi]/R^5, \tag{15}$$

$$\delta B_{||}^{(z)} = 2\delta v\ m_o\ [(X_o-x)(D-z)\sin\psi + (D-z)^2\cos\psi]/R^5. \tag{16}$$

Similarly, the individual components of $\delta\underset{\sim}{B}_{\perp}$ can be obtained by expanding (12). One finds

$$\delta B_{\perp}^{(x)} = \delta v\ m_o\ [-(Y_o-y)^2\sin\psi - (D-z)^2\sin\psi + (X_o-x)(D-z)\cos\psi]/R^5, \tag{17}$$

$$\delta B_{\perp}^{(y)} = \delta v\ m_o\ [(X_o-x)(Y_o-y)\sin\psi + (Y_o-y)(D-z)\cos\psi]/R^5, \tag{18}$$

$$\delta B_{\perp}^{(z)} = \delta v\ m_o\ [(X_o-x)(D-z)\sin\psi - (X_o-x)^2\cos\psi - (Y_o-y)^2\cos\psi]/R_5. \tag{19}$$

The total magnitude of any one of the above components, which we represent as $B_J^{(k)}$, is then obtained by replacing Δv by dxdydz and integrating over all possible volume elements containing magnetic material. This leads to the form

$$B_J^{(k)} = \iiint dxdydz\ \delta\ B_J^{(k)}. \tag{20}$$

in which $\delta B_J^{(k)}$ represents any one of the expressions (14) to (19) with Δv excluded. The limits of integration range over all of the distributed magnetic material. Upon performing the integration over some known or assumed distribution of magnetic material, one obtains the total for any component in the form

$$B^{(k)} = B_{||}^{(k)} + B_{\perp}^{(k)}. \tag{21}$$

B. Spherical Distributions

When the magnetic material is distributed over a spherical distribution of cracks, voids, and fissures in the rocks, having an effective radius $r = \rho$, measured from the origin 0 of Fig. 2, we can replace x, y, z of (14) to (19) by equivalent spherical coordinates. In this case R in (13) becomes

$$R = (R_o^2 + r^2 - 2X_o r \sin\theta \cos\phi - 2Y_o r \sin\theta \sin\phi - 2Dr \cos\theta)^{1/2}. \tag{22}$$

Since $R_o^2 = X_o^2 + Y_o^2 + D^2$ and r is always $< R_o$ or D, the total value of the last four terms inside the parentheses will always be small compared to R_o. Consequently, the expansion of R^{-5} in (11) and (12) is valid and can be expressed in the form

$$\begin{aligned} R^{-5} = R_o^{-5} [1 &- (5/2)(r^2 - 2X_o r \sin\theta \cos\phi - 2Y_o r \sin\theta \sin\phi \\ &- 2Dr \cos\theta)/R_o^2 + (35/8R_o^4)(r^4 + 4X_o^2 r^2 \sin^2\theta \cos^2\phi + 4Y_o^2 r^2 \sin^2\theta \sin^2\phi \\ &+ 4D^2 r^2 \cos^2\theta - 4X_o r^3 \sin\theta \cos\phi - 4Y_o r^3 \sin\theta \sin\phi - 4Dr^3 \cos\theta \\ &+ 8X_o Y_o r^2 \sin^2\theta \sin\phi \cos\phi + 8X_o Dr^2 \sin\theta \cos\theta \cos\phi \\ &+ 8Y_o Dr^2 \sin\theta \cos\theta \sin\phi) + \ldots] . \end{aligned} \tag{23}$$

If we now substitute (23) into (14) to (19), replace Δv by $r^2 \sin\theta \, dr \, d\theta \, d\phi$, x by $r \sin\theta \cos\phi$, y by $r \sin\theta \sin\phi$, z by $r \cos\theta$ and integrate r from 0 to ρ, θ from 0 to π, ϕ from 0 to 2π, we obtain an expression for each of the six field components indicated symbolically by (20). The integrations are lengthy; e.g., for Eq. (14), 60 separate integrations are involved. However only a

few types of integrations are involved and, in many cases, the integrations over θ and ϕ lead to zero result. Although it is necessary to perform the integrations over terms of $0(r^7/R_o^7)$ because some reduce to $0(r^5/R_o^5)$, we will finally retain only terms of $0(r^5/R_o^5)$. One reaches the point where the integrations can be done by inspection.

Performing these integrations leads to the following results:

$$B_{||}^{(x)} = (8\pi m_o \rho^3/3R_o^3)\ [X_o(X_o \sin\psi + D\cos\psi)/R_o^2 + \rho^2 \sin\psi/5R_o^2], \tag{24}$$

$$B_{||}^{(y)} = (8\pi m_o \rho^3/3R_o^3)\ [Y_o(X_o \sin\psi + D\cos\psi)/R_o^2]. \tag{25}$$

$$B_{||}^{(z)} = (8\pi m_o \rho^3/3R_o^3)\ [D(X_o \sin\psi + D\cos\psi)/R_o^2 + \rho^2 \cos\psi/5R_o^2]. \tag{26}$$

$$B_{\perp}^{(x)} = (4\pi m_o \rho^3/3R_o^3)\ [DX_o \cos\psi - (Y_o^2 + D^2 + 2\rho^2/5) \sin\psi]/R_o^2. \tag{27}$$

$$B_{\perp}^{(y)} = (4\pi m_o \rho^3/3R_o^3)\ (X_o Y_o \sin\psi + Y_o D\cos\psi)/R_o^2. \tag{28}$$

$$B_{\perp}^{(z)} = (4\pi m_o \rho^3/3R_o^3)\ [DX_o \sin\psi - (X_o^2 + Y_o^2 + 2\rho^2/5) \cos\psi]/R_o^2. \tag{29}$$

In most cases terms of $0(r^5/R_o^5)$ which are retained above will be negligible since the maximum effective ρ is not expected to exceed about $0.25\ R_o$. Combining (24) with (27), (25) with (28), and (26) with (29) leads to the total field components,

$$B_x = (4\pi m_o \rho^3/3R_o^5)\ [(2X_o^2 - Y_o^2 - D^2) \sin\psi + 3X_o D\cos\psi], \tag{30}$$

$$B_y = (4\pi m_o \rho^3/3R_o^5)\ (3Y_o)\ (X_o \sin\psi + D\cos\psi), \tag{31}$$

$$B_z = (4\pi m_o \rho^3/3R_o^5)\ [(2D^2 - X_o^2 - Y_o^2) \cos\psi + 3X_o D \sin\psi]. \tag{32}$$

These results are all derivable from the single function, the scalar magnetic potential

$$V = (4\pi m_o \rho^3/3R_o^3)(X_o \sin\psi + D\cos\psi). \tag{33}$$

by simply taking the derivatives $(-\partial V/\partial X_o) = B_x$, $(-\partial V/\partial Y_o) = B_y$ and $(-\partial V/\partial D) = B_z$. Note that after completing the integrations, the dimensions remain the same, i.e., B_x in (30) has the same units, Oe, as m_o while the scalar magnetic potential function V has the units Oe-cm.

C. Wedge Distributions

The actual hydrofractured zone is more likely to be a narrow split in the rock that may be only a few millimeters wide. However, it can be expected to extend as much as 300 m outward from the bottom of the borehole. Because the borehole is itself vertical, the split is most likely to have a vertical orientation. Thus, we can think of one or more thin sheets spreading outward from the borehole that are to be flooded with magnetic material. This situation can be represented by a mathematical approximation based on the same spherical coordinate formulation given in the previous section. As depicted in Fig. 4, one fixes the azimuthal angle ϕ at some arbitrary value and then one represents the split by picking some small appropriate angle $\Delta\phi$. The integration is then performed as before by integrating over the polar angle θ and radius r out to $r = \rho$.

The magnetic field components at the surface due to such a distribution of polarizable material are as follows:

$$B_{||}^{(x)} = (2m_o\Delta\phi\rho^3/R^3)\left\{2X(X\sin\psi + D\cos\psi)/(3R^2) + (\pi\rho/8R)\right.$$
$$X\,[5(D\cos\psi + X\sin\psi)(X^2\cos\phi + XY\sin\phi)/R^3$$
$$\left. - \cos\phi\,(D\cos\psi + 2X\sin\psi)/R]\right\}\ , \qquad (34)$$

$$B_{||}^{(y)} = (2m_o\Delta\phi\rho^3/R^3)\left\{2Y(X\sin\psi + D\cos\psi)/3R^2 + (\pi\rho/8R)\right.$$
$$X\,[5Y(D\cos\psi + X\sin\psi)(X\cos\phi + Y\sin\phi)/R^3$$
$$\left. - \sin\phi\,(D\cos\psi + X\sin\psi)/R - Y\cos\phi\,\sin\psi/R]\right\}\ , \qquad (35)$$

$$B_{||}^{(z)} = (2m_o\Delta\phi\rho^3/R^3)\left\{2D(D\cos\psi + X\sin\psi)/R^2 + (\pi\rho/8R)\right.$$
$$X\,[5D(D\cos\psi + X\sin\psi)(X\cos\phi + Y\sin\phi)/R^3$$
$$\left. - D\sin\psi\,\cos\phi/R]\right\}\ , \qquad (36)$$

$$B_{\perp}^{(x)} = (m_o \Delta\phi \rho^3/R^3) \left\{ 2(DX \cos\psi - Y^2 \sin\psi - D^2 \sin\psi)/R^2 + (\pi\rho/8R) \right.$$

$$X \left[5(DX \cos\psi - Y^2 \sin\psi - D^2 \sin\psi)(X \cos\phi + Y \sin\phi)/R^3 \right.$$

$$\left. \left. - D \cos\psi \cos\phi/R + 2Y \sin\psi \sin\phi/R \right] \right\} \cdot \qquad (37)$$

$$B_{\perp}^{(y)} = (m_o \Delta\phi \rho^3/R^3) \left\{ 2Y(D \cos\psi + X \sin\psi) + (\pi\rho/8R) \right.$$

$$X \left[5Y(D \cos\psi + X \sin\psi)(X \cos\phi + Y \sin\phi)/R^3 \right.$$

$$\left. \left. - (D \cos\psi \sin\phi + X \sin\psi \sin\phi + Y \sin\psi \cos\phi)/R \right] \right\} \cdot \qquad (38)$$

$$B_{\perp}^{(z)} = (m_o \Delta\phi \rho^3/R^3) \left\{ 2(DX \sin\psi - X^2 \cos\psi - Y^2 \cos\psi)/R^2 + (\pi\rho/8R) \right.$$

$$X \left[5(DX \sin\psi - Y^2 \cos\psi - X^2 \cos\psi)(X \cos\phi + Y \sin\phi)/R^3 \right.$$

$$\left. \left. + (2X \cos\phi \cos\psi + 2Y \sin\phi \cos\psi - D \cos\phi \sin\psi)/R \right] \right\} \cdot \qquad (39)$$

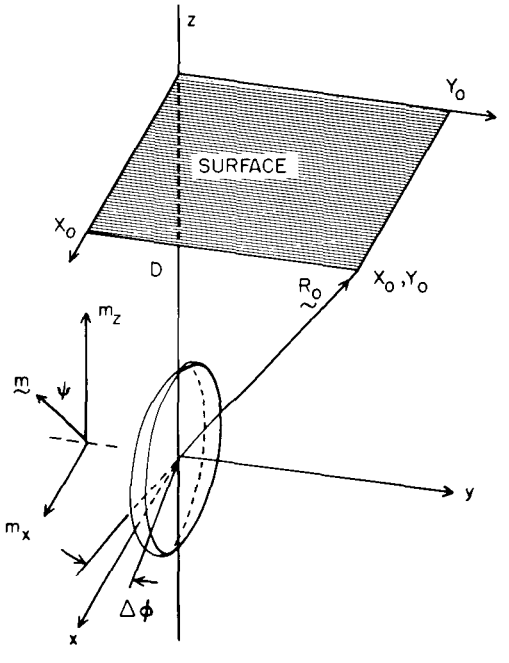

Fig. 4.
Illustration of a $\Delta\phi$ wedge distribution as an approximation to an actual crack produced by hydrofracturing. Angle ϕ of orientation of above wedge is 0°. However, calculations can be done for any $0° \leq \phi \leq 360°$. Wedge with $\Delta\phi = 1.5 \times 10^{-5}$ radians and radius of 300 m corresponds to crack with width of 2 mm and radius 300 m.

In the above results we have omitted the subscripts on X, Y, D for convenience. We have omitted also terms of $0(\rho^5/R^5)$ that were retained in (24) to (29). However, when we integrated (24) to (29) to obtain the total field components, the terms of $0(\rho/R^5)$ vanished, and no terms of $0(\rho^4/R^4)$ were present because they disappeared upon integration over ϕ from 0 to 2π. The terms of $0(\rho^4/R^4)$ will not disappear when we now combine (34) to (38) to give the field components for the wedge. Ordinarily, we would omit terms of $0(\rho^4/R^4)$ but in the case of a magnetometer lowered into the borehole, (ρ/R) could have a value possibly between 0.4 and 0.9 and therefore, these terms could make a significant contribution to the total field.

Summing (34) to (38), we find for the net field components

$$B_x = (2m_o\Delta\phi\rho^3/R^3)[3DX\cos\psi + (2X^2 - Y^2 - D^2)\sin\psi]/3R^2$$

$$+ (m_o\Delta\phi\rho^4/R^4)[-3\,(D\cos\psi\cos\phi + 3X\sin\psi\cos\phi + Y\sin\psi\sin\phi)/(8R)$$

$$+ 15X\,(D\cos\psi + X\sin\psi)(X\cos\phi + Y\sin\phi)/(8R^3)]\,, \tag{40}$$

$$B_y = (2m_o\Delta\phi\rho^3/R^3)[Y(D\cos\psi + X\sin\psi)/R^2]$$

$$+ (m_o\Delta\phi\rho^4/R^4)[-3\,(D\cos\psi\sin\phi + X\sin\psi\sin\phi + Y\sin\psi\cos\phi)/(8R)$$

$$+ 15Y\,(D\cos\phi + X\sin\psi)(X\cos\phi + Y\sin\phi)/(8R^3)]\,, \tag{41}$$

$$B_z = (2m_o\Delta\phi\rho^3/R^3)[3DX\sin\psi + (2D^2 - X^2 - Y^2)\cos\psi]/3R^2$$

$$+ (m_o\Delta\phi\rho^4/R^4)[-3\,(D\sin\psi\cos\phi + X\cos\psi\cos\phi + Y\cos\psi\sin\phi)/(8R)$$

$$+ 15D\,(D\cos\psi + X\sin\psi)(X\cos\phi + Y\sin\phi)/(8R^3)]\,. \tag{42}$$

The above results can be derived from the scalar magnetic potential function

$$V = (2m_o\Delta\phi\rho^3/3)(D\cos\psi + X\sin\psi)/R^3$$

$$+ (m_o\Delta\phi\rho^4/8)[3\,(D\cos\psi + X\sin\psi)(X\cos\phi + Y\sin\phi)/R^5$$

$$- \sin\psi\cos\phi/R^3] \tag{43}$$

by taking the derivatives $(-\partial V/\partial X)$, $(-\partial V/\partial Y)$, and $(-\partial V/\partial D)$. This procedure provides an internal check on the accuracy of the integrations that led to (40) to (42).

Another type of wedge distribution amenable to integration is shown in Fig. 5. In this sketch, $\theta = 90°$ while ϕ varies from about $-30°$ to $+150°$, and the "wedge" subtends a very small angle $\Delta\theta$. This sketch is merely illustrative. Actually, there is no difficulty in carrying out integrations for any arbitrary fixed angle θ. However, we shall not work out various examples here because the most probable crack or split in the rocks is more likely to be of the type that

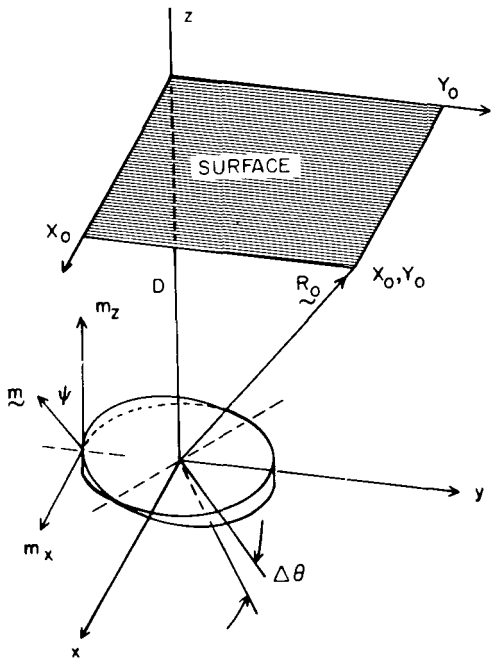

Fig. 5.
Illustration of a $\Delta\theta$ wedge distribution as an approximation to a crack produced by hydrofracturing in the horizontal plane. The angle θ for the wedge shown is 90° although calculations can be readily done for any angle.

can be represented approximately by the $\Delta\phi$ type of wedge distribution discussed above.

D. Crack Distributions

The wedge distribution of the previous section was selected for calculation because it was presumed to provide a good approximation to the magnetic fields from crack distributions, provided the wedge angle $\Delta\phi$ is chosen so that the wedge volume equals the crack volume. However, we realized later on in the analysis that it was just as easy to calculate the results for an actual crack as for a wedge, i.e., we can again use the spherical coordinate formulation. The calculations are accomplished, as before, by integrating (14) to (19) over the volume of magnetic material contained in the distribution. Previously, we have used the spherical coordinate volume element $r^2 \sin\theta\, dr\, d\theta\, d\phi$, which we write as $(r\, dr\, d\theta)(r \sin\theta\, d\phi)$. However, now for the crack, we simply replace $(r \sin\theta\, d\phi)$ by the constant width t of the thin crack, t being only of the order of a few millimeters, and integrate with respect to the area element $(r\, dr\, d\theta)$ of the semicircular area. Again, x, y, z in (14) to (19) are expressed in spherical coordinates and the limits of integration remain $0 \leq r \leq \rho$, $0 \leq \theta \leq \pi$, while ϕ remains constant. The integrations lead to the parallel and perpendicular components which must be added to give the net field components, i.e., B_x, B_y, B_z are the sums of the integrals of (14) and (17), (15) and (18), (16) and (19), respectively. The actual integrations are just as tedious as those of the previous two sections; we obtain the results,

$$B_x = (\pi m_o t\rho^2/2R_o^3)[3X_o(X_o \sin\psi + D\cos\psi)/R_o^2 - \sin\psi]$$

$$(2\, m_o t\rho^3/3R_o^4)[-(9X_o \cos\phi \sin\psi + 3\, Y_o \sin\phi \sin\psi + 3\, D \cos\phi \cos\psi)/R_o$$

$$+ 15\, X_o(X_o \cos\phi + Y_o \sin\phi)(X_o \sin\psi + D\cos\psi)/R_o^3], \qquad (44)$$

$$B_y = (\pi m_o t\rho^2/2R_o^3)[3Y_o(X_o \sin\psi + D\cos\psi)/R_o^2]$$

$$+ (2\, m_o t\rho^3/3R_o^4)[-3\,(X_o \sin\phi \sin\psi + Y_o \cos\phi \sin\psi + D \sin\phi \cos\psi)/R_o$$

$$+ 15Y_o\,(X_o \cos\phi + Y_o \sin\phi)(X_o \sin\psi + D\cos\psi)/R_o^3], \qquad (45)$$

$$B_z = (\pi m_o t\rho^2/2R_o^3)[3D\,(X_o \sin\psi + D\cos\psi)/R_o^2 - \cos\psi]$$

$$+ (2\, m_o t\rho^3/3R_o^4)[-3(X_o \cos\phi \cos\psi + Y_o \sin\phi \cos\psi + D\cos\phi \sin\psi)/R_o$$

$$+ 15\, D\,(X_o \cos\phi + Y_o \sin\phi)(X_o \sin\psi + D\cos\psi)/R_o^3]. \qquad (46)$$

In the above, terms of order (ρ^4/R^4), (ρ^5/R^5), etc., have been neglected.

It is useful to determine the scalar magnetic potential function from which B_x, B_y, B_z can be derived. This is a valuable exercise in that it provides an independent check on the accuracy of the above integrations. We find for this function

$$V = (\pi m_o t\rho^2/2)[(X \sin\psi + Z\cos\psi)/R^3]$$

$$+ (2\, m_o t\rho^3/3)[3\,(X\cos\phi + Y\sin\phi)(X\sin\psi + Z\cos\psi)/R^5$$

$$- \cos\phi \sin\psi\, /R^3], \qquad (47)$$

the negative derivatives of which give the same results as in (44) to (46), when evaluated at $X = X_o$, $Y = Y_o$, $Z = D$.

A comparison of the results (40) - (42) for the wedge distribution with (44) - (46) for the crack distribution is quite surprising. In the former the part containing the orientation angle ϕ is $\sim (\rho^4/R_o^4)$, whereas for the crack distribution this part is $\sim (\rho^3/R_o^3)$. However, as we shall see later, the final nu-

merical results for assumed equivalent cases are not significantly different. Therefore, the use of the wedge approximation to the crack distribution turns out a good and useful approximation, especially for the case of measurements by magnetometers and gradiometers situated in the borehole itself.

IV. FIELDS IN THE BOREHOLE NEAR LOCAL DISTRIBUTIONS

A. General

The fields produced by the polarization of magnetic material forced into a crack produced by hydrofracturing can be estimated for instrument locations near the bottom of the borehole. We shall assume that the material in such a crack will exhibit fields similar to those due to a uniform distribution of magnetic material in a wedge such as that shown in Fig. 4. Let the wedge be at any arbitrary angle ϕ, rather than at $\phi = 0$ degrees as in Fig. 4, and subtend a very small angle $\Delta\phi$. The volume of such a wedge is $2\Delta\phi(\rho^3/3 - r_m^3/3)$, where ρ and r_m are the maximum and minimum radii of the distribution, respectively. Since an actual crack produced by hydrofracturing may have a width of only a few millimeters and an extent of 100 to 300 m, we would pick ρ = 100 to 300 m, $0 < r_m <$ a few m, and adjust $\Delta\phi$ so that the volume of the wedge is the same as that of the crack. We calculate the fields for such a wedge distribution in IV. B below.

It is important at this point to call attention to a very real problem that will be encountered in all measurements by magnetometers or gradiometers located in the borehole. As we shall see in the next section, the magnetometer and gradiometer signal formulas carry prefactors of the forms $\log(\rho/r_m)$ and $(1/r_m - 1/\rho)$, respectively. These prefactors indicate the possibility of logarithmic or $1/r_m$ singularities as $r_m \to 0$. However, this will not occur in practice because the housing of these instruments will always preclude $r_m = 0$. Nevertheless, when a cylindrical shell of magnetic material surrounds the instrument housing in the bottom of the borehole, r_m will be small and the magnetic signal will exhibit a very large omnidirectional component. This will tend to obscure the directional information that might otherwise be provided by magnetic material located in the crack or fracture some distance away from the bottom of the borehole. It should be possible to eliminate this problem in practice by eliminating the cylindrical shell of magnetic material in the bottom portions of the borehole. The obvious way to do this is to pump in a suitably small amount of nonmagnetic material immediately after flooding the borehole plus cracks and fractures with magnetic material. This process should push the minimum radius r_m out to an acceptable dis-

tance of a few m while eliminating, at the same time, the undesirable omnidirectional signal component.

B. Fields Due to Local Wedge Distributions

A superconducting gradiometer with axis in the x-y plane will sense field components at points described by the vectors $\underset{\sim}{S}$ and $-\underset{\sim}{S}$ measured with respect to the central (vertical) axis of the borehole, where $2|\underset{\sim}{S}|$ is < borehole diameter. Thus, we wish to evaluate the field components, as given by (14)-(19) at a point $X_o = S\cos\chi$, $Y_o = S\sin\chi$, $Z_o = d$, where χ is the azimuthal angle of the point, measured with respect to the x-axis in Fig. 4, and $d < \rho$ (ρ = the maximum radius of the distribution of magnetic material). Thus, the terms $(X_o - x)$, $(Y_o - y)$, $(D - z)$, in the numerators of (14)-(19) can then be expressed in spherical coordinates in the forms

$$\begin{aligned} &- (r\sin\theta\cos\phi - S\cos\chi), \\ &- (r\sin\theta\sin\phi - S\sin\chi), \\ &- (r\cos\theta - d), \end{aligned} \tag{48}$$

respectively. The distance from the point ($S\cos\chi$, $S\sin\chi$, d) to a volume element containing magnetic material is then

$$R = (r^2 + d^2 + S^2 - 2rS\sin\theta\cos\phi\cos\chi - 2rS\sin\theta\sin\phi\sin\chi - 2rd\cos\theta)^{1/2}. \tag{49}$$

Substituting (48), (49), into (14)-(19) and integrating over the wedge distribution then gives the desired field components. However, when $S < d < \rho$, the integrands will contain singularities. In such cases one can carry out the transformation to complex variable form, determine the poles of the integrands, and perform the integrations by summation of residues. Unfortunately, this involves a number of branch cuts and the summation of residues on at least five Riemann sheets. Since this is rather complicated, we will not do this aspect of the problem in the present report. On the other hand, very useful and meaningful information can be obtained by simplifying the problem in the following way: Let $d = 0$ and S be $< r_m$, where r_m is the minimum radius achieved in practice as described in the previous section. In this case, the simple expansion of R^{-5} is valid and leads to

$$R^{-5} = (r^2 + S^2)^{-5/2}[1-2rS\sin\theta\cos(\chi - \phi)/(r^2 + S^2)]^{-5/2}$$

$$= (r^2 + S^2)^{-5/2} + 5\,rS\sin\theta\cos(\chi - \phi)(r^2 + S^2)^{-7/2} + \ldots$$

$$\approx r^{-5} + 5\,r^{-6}S\sin\theta\cos(\chi - \phi) - r^{-5}0\,(S^2/r^2) + \ldots\,. \qquad (50)$$

Substitution of (48)-(50) into (14)-(19) and integrating (r ranges from r_m to ρ, θ from 0 to 2π), we obtain

$$B_{||}^{(x)} = 2\,m_o\Delta\phi\,\sin\psi\left\{(4/3)\cos^2\phi\,\log(\rho/r_m) + \pi(1/\rho - 1/r_m)\right.$$

$$\left. X[S\cos\chi\cos\phi - (15/8)\,S'\cos^2\phi]\right\}. \qquad (51)$$

$$B_{||}^{(y)} = 2\,m_o\Delta\phi\,\sin\psi\left\{(4/3)\,\sin\phi\cos\phi\,\log(\rho/r_m) + \pi(1/\rho - 1/4_m)\right.$$

$$\left. X[(S/2)\sin(\chi + \phi) - (15/8)S'\sin\phi\cos\phi]\right\}. \qquad (52)$$

$$B_{||}^{(z)} = 2\,m_o\Delta\phi\,\cos\psi\left\{(2/3)\,\log(\rho/r_m) - (5\pi/8)(1/\rho - 1/r_m)S'\right\}. \qquad (53)$$

$$B_{\perp}^{(x)} = m_o\Delta\phi\,\sin\psi\left\{-(2/3)(2\sin^2\phi + 1)\,\log(\rho/r_m) + \pi(1/\rho - 1/r_m)\right.$$

$$X[-S\sin\phi\sin\chi + (15/8)S'\sin^2\phi\cos(\chi - \phi)$$

$$\left. + (5/8)S'\cos(\chi - \phi)]\right\}. \qquad (54)$$

$$B_{\perp}^{(y)} = m_o\Delta\phi\,\sin\psi\left\{(4/3)\sin\phi\cos\phi\,\log(\rho/r_m) + \pi(1/\rho - 1/r_m)\right.$$

$$\left. X[(S/2)\sin(\chi + \phi) - (15/8)S'\sin\phi\cos\phi]\right\}. \qquad (55)$$

$$B_{\perp}^{(z)} = m_o\Delta\phi\,\cos\psi\left\{-(4/3)\log(\rho/r_m) + \pi(1/\rho - 1/r_m)\right.$$

$$\left. X[-S\cos\chi\cos\phi + (15/8)S'\cos^2\phi - (15/8)S'\sin^2\phi]\right\}. \qquad (56)$$

where $S' = S\cos(\chi - \phi)$.

The net x-component is therefore the sum $B_x = B_{||}^{(x)} + B_{\perp}^{(x)}$: similarly, one obtains B_y and B_z. However, a directional magnetometer and/or a gradiometer loop located at the point ($S\cos\chi$, $S\sin\chi$, $z = 0$) will measure the field $B_x\cos\chi + B_y\sin\chi$. Combining the above results we therefore obtain

$$B_x\cos\chi + B_y\sin\chi = m_o\Delta\phi \sin\psi \log(\rho/r_m) [4 \cos\phi \cos(\chi - \phi) - 2 \cos\chi]$$

$$- S \sin\psi (\pi m_o\Delta\phi/8)(1/r_m - 1/\rho) [12 \cos\phi$$

$$+ 24 \cos\chi \cos(\chi - \phi) - 45 \cos\phi \cos(\chi - \phi)]. \qquad (57)$$

When we put S = 0, we obtain the directional signal that would be measured by a magnetometer oriented in the x-y plane at the angle χ. On the other hand, if we replace S in (57) by (-S), and subtract (57) from this result, we obtain the signal that would be measured by a superconducting gradiometer with its axis in the x-y plane and oriented at the angle χ. In this latter case, the leading terms would cancel and we would have a result equal to twice the second term of (57).

Since m_o, $\Delta\phi$, ρ/r_m, and wedge orientation angle ϕ are fixed for any given distribution, the signal variation measured by a magnetometer that is rotated in the x-y plane to the angle χ is given by

$$B_m(\chi) = H_h\cos\chi + m_o\Delta\phi \sin\psi \log(\rho/r_m) [4 \cos\phi \cos(\chi - \phi) - 2 \cos\chi] \qquad (58)$$

where H_h = 0.2199 G as given by (3), is the horizontal component of the earth's field. The $H_h\cos\chi$ term in (58) could, in actual practice, dominate and obscure the local anomaly signal expressed by the second part of (58) and thereby eliminate the directional information contained in the square brackets of (58). We propose in the next section a new data processing method that employs a second identical magnetometer that is always synchronized to the same angle χ. It will be sufficiently far away from the borehole anomaly so that the anomaly part of its signal is negligible. Subtracting the signals from these two magnetometers should then give a signal that is essentially the second part of (58), except for magnetic noise.

The magnetometer anomaly directional function [2 $\cos\phi \cos(\chi - \phi)$ - $\cos\chi$], which is one-half the function in the square brackets of (58), is shown in Fig. 6 plotted as a function of χ for 24 different specific values of ϕ (for every 15 degrees). Assuming that the $H_h\cos\chi$ part of the experimental magnetometer signal can be subtracted away, as suggested above, then the remaining anomaly signal can be computer-analyzed by cross-correlation with the function [2 $\cos\phi \cos(\chi - \phi)$ - $\cos\chi$], over all χ from 0 to 360°. This cross-correlation will have a maximum

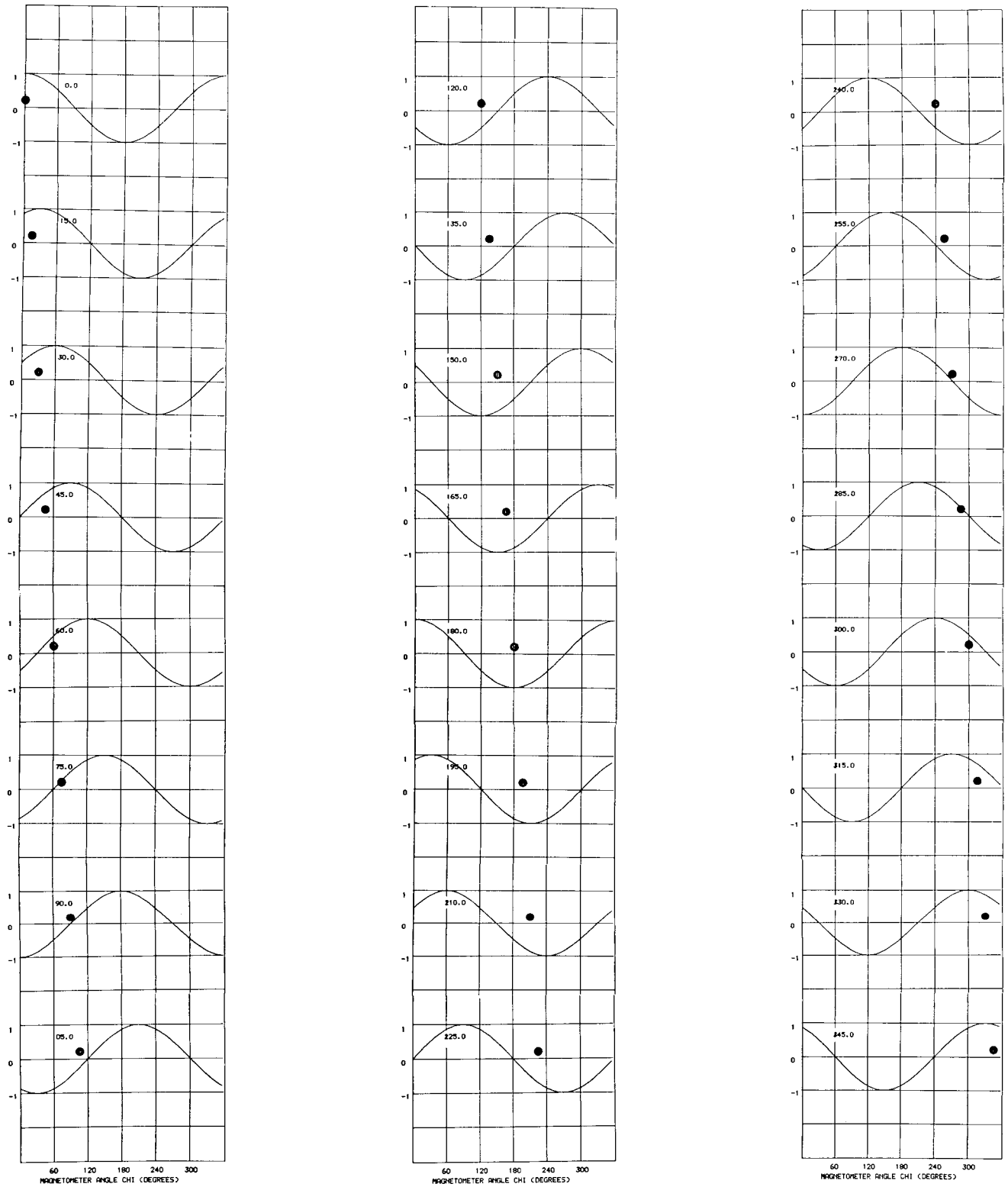

Fig. 6.

Normalized response of a direction-sensitive borehole magnetometer, with axis in the x-y plane, at position X = Y = Z = 0 as a function of angle of rotation χ. The orientation of the magnetic anomaly (represented by a wedge distribution of very small angle $\Delta\phi$) varies from $\phi = 0°$ to $\phi = 345°$ in steps of 15°. Note that response at any given ϕ is the same as that at $\phi + 180°$. Thus, the directional magnetometer response is troubled by a 180° ambiguity.

value when this test function has the correct angle ϕ. Thus, by this method one might be able to estimate the direction ϕ of the crack produced by hydrofracture.

Using the result (57) and differentiating H_h as given by (1) we obtain the signal that should be observed by a gradiometer oriented to the angle χ. This signal has the form

$$\Delta B_g(\chi) = (2S/a)\, H_o(d \sin\theta_e/d\mu)\cos\chi - 2S \sin\psi\, (\pi m_o \Delta\phi/8)(1/r_m - 1/\rho)$$

$$\times [12 \cos\phi + 24 \cos\chi \cos(\chi - \phi) - 45 \cos\phi \cos(\chi - \phi)], \quad (59)$$

where θ_e is the function θ of (1), as defined in terms of the geomagnetic co-latitude μ in (2). Differentiating (2), we obtain for the leading term of (59),

$$- (2S/a)\, H_o(a/r)^3(\cos\theta_e/\sin\theta_e)\, [-\sin\mu \cos\mu_o$$

$$+ \cos\mu \sin\mu_o \cos(\lambda - \lambda_o)] \cos\chi. \quad (60)$$

A superconducting gradiometer loop spacing (2S) suitable for borehole application would be about 2.0 cm, and since a in (1) is 6.371×10^8 cm, the prefactor (2S/a) is 0.314×10^{-8}. It is of interest to evaluate this undesirable earth's field contribution to the overall gradiometer signal for the same geographical location discussed in Sec. II. A. Using the values of μ, μ_o, λ, and λ_o, and $H_o = 0.3035$ Oe, we obtain for (60)

$$0.95 \times 10^{-9} \cos\chi \text{ (Oe)}, \quad (61)$$

which is about ten times the sensitivity of a 30-MHz SQUID sensor.

The contribution to the gradiometer signal arising from the local anomaly should be considerably greater than (61) in order to be able to distinguish it via the type of computer cross-correlation analysis discussed above. If we use a paramagnetic fluid, rather than a ferromagnetic slurry, the anomaly signal will be of the same magnitude as (61). It will therefore be necessary to remove this earth's field contribution before doing the cross-correlation analysis of the experimental rotation data. This can be accomplished, in a manner similar to that already described, by having a second identical gradiometer system on the

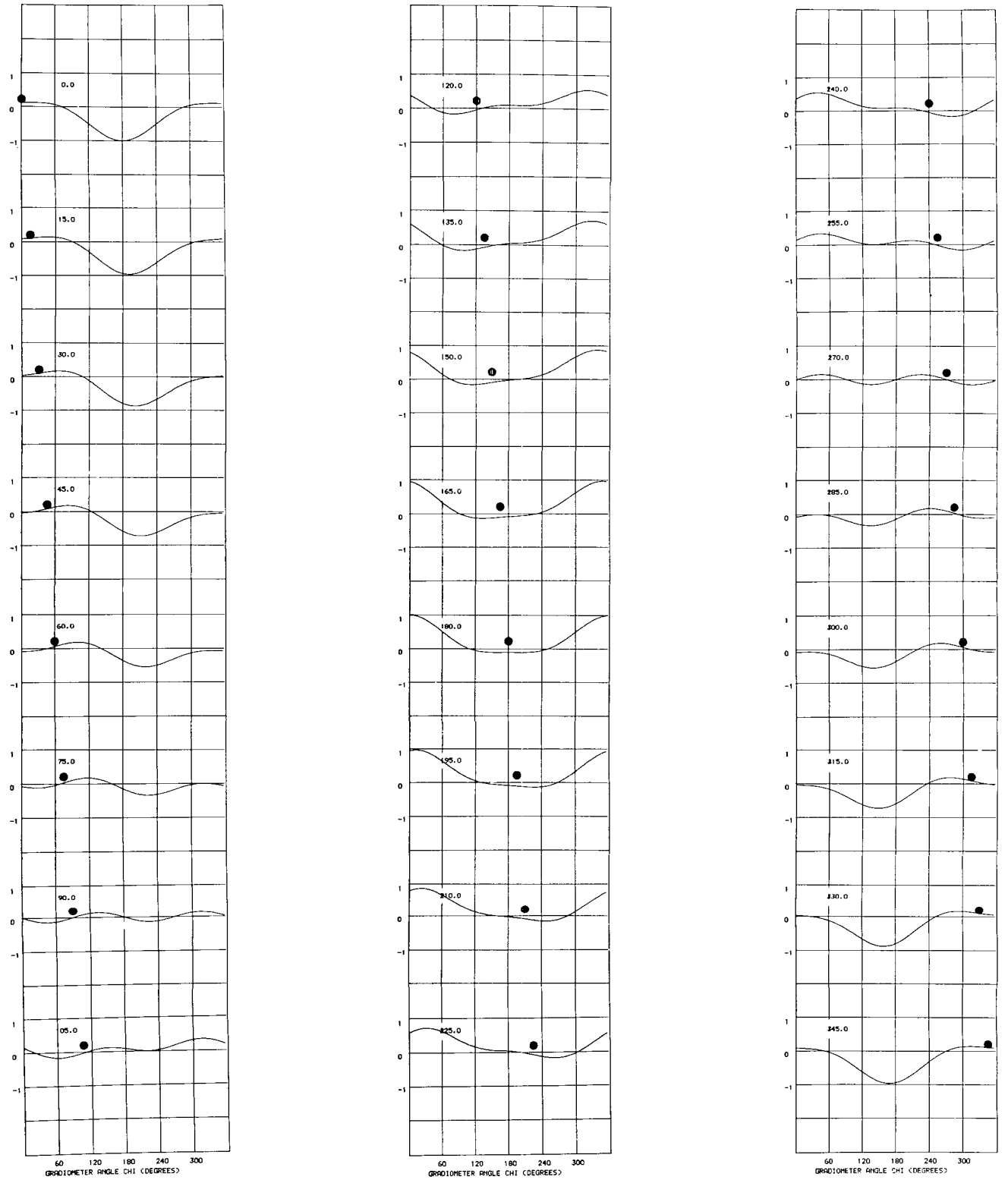

Fig. 7.

Normalized response of an axial-type superconducting gradiometer with its axis in the x-y plane as a function of rotation angle χ. These are plots of the function (63) in which the orientation ϕ' of the magnetic anomaly (represented by a wedge distribution of very small angle $\Delta\phi$) varies from $\phi' = 0°$ to $\phi = 345°$ in 15° steps. The response at any given ϕ' is different from that at $\phi' + 180°$. Thus, the borehole gradiometer is capable of resolving the 180° ambiguity of Fig. 6.

surface that is rotated to the same angle χ in synchronism with the rotation of the borehole gradiometer. When the two signals are subtracted in a data acquisition system, the end result will be the signal

$$\Delta B_g(\chi) = -(2S)\sin\psi\,(\pi m_o \Delta\phi/8)(1/r_m - 1/\rho)\,[12\cos\phi + 24\cos\chi\cos(\chi - \phi) - 45\cos\phi\cos(\chi - \phi)] + \Delta B_N(\chi), \tag{62}$$

where $\Delta B_N(\chi)$ is the magnetic gradient noise component of the gradiometer signal.

If ϕ is the actual angular orientation of the crack or fracture, the signal (62) can be cross-correlated with the normalized function

$$f(\phi') = [12\cos\phi' + 24\cos\chi\cos(\chi - \phi')] - 45\cos\phi'\cos(\chi - \phi')]/81, \tag{63}$$

in which the division by 81 normalizes the function to have a maximum value of unity. The function $f(\phi')$ is shown in Fig. 7 for 24 fixed values of ϕ' as a function of χ for $0 \leqslant \chi \leqslant 360°$. Comparing this function with the magnetometer function of Fig. 6, one sees that the gradiometer function exhibits considerably more structure than the former. Thus, one should be able to determine the angle ϕ with greater accuracy by using the gradiometer system.

V. THE ANOMALY SIGNALS DETECTED BY BOREHOLE INSTRUMENTS

A. Signals Detected by Magnetometer

The signal that will be produced in a direction-sensitive magnetometer such as a superconducting single loop or a flux gate magnetometer will arise from the sum of the contributions

$$B_j^{(c)} = B_{e,j}^{(c)} + B_{N,j}^{(c)} + B_{A,j}^{(c)}, \tag{64}$$

where $B_{e,j}$ is the steady part of the jth component of the earth's field, $B_{N,j}$ is the magnetic noise, and $B_{A,j}$ is the small additional field due to the local magnetic anomaly. The axis of the magnetomer is assumed oriented in the jth direction and it is convenient to let j = 1,2,3 correspond to the x,y,z axes of Figs. 2, 4. We use in the superscript the label (c) to denote the initial, (c) = (i), configuration of the fields prior to pumping the magnetic material into the fracture and the final, (c) = (f), configuration afterwards.

Thus, an experimental quantity that could be used to indicate the existence and properties of the anomaly is the difference $B_j^{(f)} - B_j^{(i)}$ between the initial and final observations, e.g.,

$$\Delta B_j = B_{e,j}^{(f)} - B_{e,j}^{(i)} + B_{N,j}^{(f)} - B_{N,j}^{(i)} + B_{A,j}^{(f)} . \tag{65}$$

Presumably, the anomaly prior to flooding the fractures with magnetic material will be absent so that $B_{A,j}^{(i)} = 0$.

The steady components of the earth's field should not change, even over a period of several hours, so that $B_{e,j}^{(i)}$ and $B_{e,j}^{(f)}$ can be set equal to the average value. Consequently, the leading term of (65) is zero, or, if not, the small difference can be lumped into the second square brackets of (65) as magnetic noise. Thus, ΔB_j should take the form

$$\Delta B_j = \left[B_{N,j}^{(f)} - B_{N,j}^{(i)} \right] + B_{A,j}^{(f)} . \tag{66}$$

Because of practical considerations, several hours of time may elapse before the final measurements (f) can be performed. Since $B_{N,j}^{(f)}$, $B_{N,j}^{(i)}$ contain parts due to the diurnal variation of the earth's field, the difference represented by the square brackets of (66) could amount to several tens of gammas or even as much as 100γ. This noise difference contribution could easily dominate the anomaly signal $B_{A,j}$ so that its extraction from the overall signal difference would be difficult or impossible. However, it should be possible to alleviate this difficulty if one uses a special scheme for measurement and data processing, such as that described below.

As mentioned in the preceding section, we propose to use simultaneously two nearly identical directional magnetometers having gamma-level or 0.1-gamma-level sensitivities with axes oriented in the x-y plane. One would be in the borehole at various depths (depth above anomaly center near bottom of borehole denoted by d) and the other would be on the surface (z-coordinate = D). Both would be rotated in the x-y plane so as to be simultaneously at the same angle χ, which is measured with respect to the isogonic line (x-axis of Fig. 2). Thus, the initial signals detected by the two magnetometers would have the forms

$$B^{(i,b)}(\chi) = \left[B_{e,x}^{(i,s)} + (\partial B_{e,x}/\partial z)(D - d)\right] \cos\chi$$

$$+ \left[B_{N,x}^{(i,s)} + (\partial B_{N,x}/\partial z)(D - d)\right] \cos\chi$$

$$+ \left[B_{N,y}^{(i,s)} + (\partial B_{N,y}/\partial z)(D - d)\right] \sin\chi \ , \tag{67}$$

$$B^{(i,s)}(\chi) = B_{e,x}^{(i,s)}\cos\chi + B_{N,x}^{(i,s)}\cos\chi + B_{N,y}^{(i,s)}\sin\chi \ , \tag{68}$$

in which superscripts (i,b) and (i,s) represent (initial, borehole) and (initial, surface), respectively. Note that the earth's field and noise field contributions are expressed in (67) in terms of first-order Taylor's expansions with respect to (i,s).

After flooding the fractures with magnetic material, the two signals detected by the magnetometers would have the forms,

$$B^{(f,b)}(\chi) = \left[B_{e,x}^{(f,s)} + (\partial B_{e,x}/\partial z)(D - d)\right] \cos\chi$$

$$+\left[B_{N,x}^{(f,s)} + (\partial B_{N,x}/\partial z)(D - d)\right] \cos\chi$$

$$+\left[B_{N,y}^{(f,s)} + (\partial B_{N,y}/\partial z)(D - d)\right] \sin\chi$$

$$+ B_{A,x}^{(f,b)}\cos\chi + B_{A,y}^{(f,b)}\sin\chi \ , \tag{69}$$

$$B^{(f,s)}(\chi) = B_{e,x}^{(f,s)}\cos\chi + B_{N,x}^{(f,s)}\cos\chi + B_{N,y}^{(f,s)}\sin\chi$$

$$+ B_{A,x}^{(f,s)}\cos\chi + B_{A,y}^{(f,s)}\sin\chi \ . \tag{70}$$

The experimental data would consist of the four single quantities represented by the left-hand sides of (67)-(70). These signals would be recorded on chart or magnetic tape as a function of the angle χ. At the same time, however, one can electronically obtain the differences analogous to (67) minus (68) according to

$$\Delta B^{(i)}(\chi) = B^{(i,b)}(\chi) - B^{(i,s)}(\chi)$$

$$= (\partial B^{(i)}_{e,x}/\partial z)(D - d)\cos\chi + (\partial B^{(i)}_{N,x}/\partial z)(D - d)\cos\chi$$

$$+ (\partial B^{(i)}_{N,y}/\partial z)(D - d)\sin\chi \qquad (71)$$

$$\Delta B^{(f)}(\chi) = B^{(f,b)}(\chi) - B^{(f,s)}(\chi)$$

$$= (\partial B^{(f)}_{e,x}/\partial z)(D - d)\cos\chi + (\partial B^{(f)}_{N,x}/\partial z)(D - d)\cos\chi$$

$$+ (\partial B^{(f)}_{N,y}/\partial z)\sin\chi + B^{(f,b)}_{A,x}\cos\chi + B^{(f,b)}_{A,y}\sin\chi$$

$$- B^{(f,s)}_{A,x}\cos\chi - B^{(f,s)}_{A,y}\sin\chi \,, \qquad (72)$$

In the measurement scheme we plan to locate the surface magnetometer at a sufficient distance from the local anomaly in the borehole so that the last two terms of (72) will be negligible. Therefore, the anomaly contribution to the difference $\Delta B^{(f)}(\chi)$ will be primarily that due to the last two terms of (69), i.e., that due to the local anomaly as measured by borehole magnetometer.

After the initial and final data have been obtained in the forms $\Delta B^{(i)}(\chi)$, $\Delta B^{(f)}(\chi)$ for several complete rotations of the angle χ, one can now obtain from the experimental data the second differences,

$$\Delta' B(\chi) = \Delta B^{(f)}(\chi) - \Delta B^{(i)}(\chi)$$

$$= \left[(\partial B^{(f)}_{N,x}/\partial z) - (\partial B^{(i)}_{N,x}/\partial z\right](D - d)\cos\chi$$

$$+ \left[(\partial B^{(f)}_{N,y}/\partial z) - (\partial B^{(i)}_{N,y}/\partial z)\right](D - d)\sin\chi$$

$$+ B^{(f,b)}_{A,x}\cos\chi + B^{(f,b)}_{A,y}\sin\chi \,, \qquad (73)$$

by electronic data processing. Furthermore, the computer program would perform a cross-correlation and/or an autocorrelation calculation on the second difference $\Delta B'(\chi)$. It is expected that over several cycles of the angle χ, the differences of the noise derivative contributions would randomize. Therefore, the cross-correlation and/or autocorrelation analysis should eliminate, or greatly reduce, the overall magnetic noise contribution. Thus, the net $\Delta B'(\chi)$ should closely resemble

the true value of the function of χ represented by the last two terms of (73). The above scheme and procedure for data analysis should therefore permit a reasonably accurate determination of the direction of the split in the rocks produced by hydrofracturing.

Note that the last two terms of (73) are equivalent to the last single term of (58) in the case d=0. The first term of (58) will cancel out when we use the method of data processing just described above.

We now consider the practical possibilities of the above discussion for the case in which the borehole magnetometer is located at (x=y=d=0), i.e., at the origin of Fig. 4. When the axis of this directional magnetometer is rotated in the x-y plane, it will receive a signal as given by (58) with noise components as expressed by (67) and (69). Let the local anomaly be due to a distribution of magnetic material in a crack of 2.0-mm width with radius (measured from d=0) of 100 m. Its volume is $(\pi/2)(10^8)(0.2)$ cm^3. If the corresponding wedge distribution volume $(2\pi/3)\rho^3\Delta\phi$ is to be the same, then $\Delta\phi=3(0.2)/4\rho=1.5 \times 10^{-5}$ radians. We shall choose the minimum radius r_m=2.0 m, ρ=100 m, and assume T=600 K.

We then assume for the paramagnetic case that $m_o=7.1\times10^{-5}$ Oe as given in Table 2.

For the ferromagnetic particles in slurry, we arbitrarily assume a filling factor of 0.01, a saturation polarization of 0.8 x 1760 Oe, and a remanence based on the stopping point on the hysteresis curve of 0.6. Thus, m_o = (0.6)(0.9)(1760)(0.01) = 9.5 Oe.

The factor $f_m = 2\, m_o \Delta\phi \sin\psi \log(\rho/r_m)$ is then, for a magnetometer:

$$f_m = 3.7 \times 10^{-9} \text{ Oe, paramagnetic solution;}$$

$$f_m = 5.0 \times 10^{-4} \text{ Oe, 1\% ferromagnetic particle slurry.}$$

Assuming that the signal processing can be accomplished as described above, then the final cross-correlation processing will be done on the signal

$$\Delta' B(\chi) = f_m [2 \cos\phi \cos(\chi - \phi) - \cos\chi] + \text{magnetic noise.} \qquad (74)$$

Note that f_m for the paramagnetic case is about 10^{-2} smaller than the sensitivity of the typical flux gate magnetometer but is 10 times greater than that of a 30-MHz superconducting SQUID magnetometer. Thus, the use of the paramagnetic solution is not feasible, even when the magnetometer is situated in the borehole, be-

cause a data acquisition system cannot be expected to extract a meaningful signal of $\sim 10^{-9}$ Oe out of a background of 0.3 Oe (earth's horizontal component) plus magnetic noise of 10^{-7} to 10^{-4} Oe.

On the other hand, the use of a 1% ferromagnetic particle suspension in slurry appears to be feasible because the borehole signal carrying the directional information, as expressed by (74), could be 4 to 4000 times > the expected magnetic noise amplitudes. In fact, the anomaly signal produced by 1% ferromagnetic material in slurry is large enough so that a highly directional flux gate magnetometer could be used as the sensor inasmuch as such devices have sensitivities in the range of 10^{-6} Oe. However, one would have to take pains to be sure that the surface magnetometer that is synchronized to the borehole magnetometer is fabricated to be as closely identical to the borehole unit as possible. Otherwise, the signal subtractions implied in (69) to (73) would not be valid and undesirable signal components would emerge.

In view of the above discussion, we should ask whether the direction ϕ of the crack can be determined from the single borehole magnetometer rotational measurement, which would produce a signal such as that expressed by (69). Except for noise, this signal is the same as (58) in that the last two terms of (69) are the same as the last term of (58). Thus, in the data processing, we would be attempting to extract the directional information contained in

$$f_m \left[2 \cos\phi \cos(\chi - \phi) - \cos\chi\right] , \tag{75}$$

as in (74), in the presence of the steady horizontal component, $H_h \cos\chi$ plus noise. For the ferromagnetic slurry example given above, H_h is greater than 400 f_m. Thus, no matter how sophisticated the data processing, it will be difficult to extract accurate ϕ values by computer correlations of the data. We therefore conclude that the single borehole magnetometer method would not be a feasible method for locating ϕ with the required accuracy of $\pm$ 15°.

However, we show below that the method in which the borehole magnetometer signal is simultaneously subtracted from the surface magnetometer signal can be feasible, provided the engineering requirements can be met in practice. Rather than asking that the H_h component of the borehole signal be completely subtracted from that of the surface signal, which may be difficult to do in practice, we attempt to balance to the extent that a small amount, s H_h, remains in the recorded signal. Then by reversing the surface signal, i.e., changing sign and adding, we

obtain a - s H_h component remaining in the second recorded signal. Thus, it is possible to obtain two separate signals

$$\Delta B_{+}^{(f)} = s\, H_h \cos\chi + f_m\,[2\cos\phi\cos(\chi - \phi) - \cos\chi] + \text{noise}, \tag{76}$$

$$\Delta B_{-}^{(f)} = -s\, H_h \cos\chi + f_m\,[2\cos\phi\cos(\chi - \phi) - \cos\chi] + \text{noise}. \tag{77}$$

If the signals can be balanced to the extent that s H_h is no greater than about ten times f_m, then various correlation calculations can be done successfully.

We shall consider correlations with $\sin\chi$, $\cos\chi$, and with the function $[2\cos\phi\cos(\chi - \phi) - \cos\chi]$. To best eliminate random background noise, the computer integrations should be carried over several complete cycles (0° to 360°) of the angle χ. Correlation with $\sin\chi$ leads to the numbers

$$N_{1,+} = 2\pi f_m \cos\phi \sin\phi + \text{background}_{1,+} \tag{78}$$

$$N_{1,-} = 2\pi f_m \cos\phi \sin\phi + \text{background}_{1,-}\,. \tag{79}$$

Correlation with $\cos\chi$ leads to

$$N_{2,+} = \pi s\, H_h - \pi f_m \cos 2\phi + \text{background}_{2,+} \tag{80}$$

$$N_{2,-} = -\pi s\, H_h - \pi f_m \cos 2\phi + \text{background}_{2,-}\,. \tag{81}$$

Correlation with the function $[2\cos\phi'\cos(\chi - \phi') - \cos\chi]$ leads to

$$\begin{aligned} N_{3,+} &= \pi s\, H_h(2\cos^2\phi' - 1) + \pi f_m(4\cos^2\phi'\cos^2\phi + 4\cos\phi\cos\phi'\sin\phi\sin\phi' \\ &\quad - 2\cos^2\phi' - 2\cos^2\phi + 1) + \text{background}_{3,+} \\ &= \pi s\, H_h \cos 2\phi' + \pi f_m \cos(2\phi - 2\phi') + \text{background}_{3,+}\,, \end{aligned} \tag{82}$$

$$N_{3,-} = -\pi s\, H_h \cos 2\phi' + \pi f_m \cos(2\phi - 2\phi') + \text{background}_{3,-}\,. \tag{83}$$

The maximum numerical value of the correlation calculation should result when the sum

$$N_{3,+} + N_{3,-} = 2\pi f_m \cos(2\phi - 2\phi') + 1/2 \langle \text{background} \rangle_3 \ , \tag{84}$$

has a positive maximum, i.e., then the computer input value ϕ' is equal to the anomaly orientation angle ϕ. The location of this maximum should be independent of the background noise contribution, which should be zero if we integrate over a great number of cycles of χ, provided the noise is random.

When the background contributions to the correlation functions are sufficiently small, we can calculate fairly accurately the sums $(N_{1,+} + N_{1,-})$ and $(N_{2,+} + N_{2,-})$, and calculate their ratios which is now an estimate of $\tan 2\phi$. This procedure will give an independent determination of ϕ, which should be just as accurate as that determined from the maximum value of (84), except when ϕ is close to 90° or 270°.

Unfortunately, both of these methods for determining ϕ from magnetometer data plus tricks lead to ϕ values that can be ambiguous by 180°. We can look for help toward resolving this ambiguity by examining the shape of the signal as a function of χ as shown in Fig. 6. Again, we see the 180° ambiguity in the signal itself. Consequently, although the correlation techniques lead to accurate ϕ, there is no way to avoid the 180° ambiguity by just using only a horizontally mounted rotating magnetometer. However, by tilting the plane of a second borehole magnetometer, it should be possible to resolve the ambiguity. Analysis of this system will not be done in this present work.

B. Signal by Horizontal Axial Gradiometers

The signals that will be detected by two identical gradiometers, one on the surface at a point ($X = X_o$, $Y = 0$, $Z = D$), and one at the point ($X = Y = 0$, $Z = d \approx 0$) in the borehole, respectively, can be evaluated by straightforward procedures. We consider in this section only the case in which the axes of the two axial gradiometers are always in the x-y plane and simultaneously oriented to the same angle χ, which is measured with respect to the X-axes of Figs. 2, 4, and 5. The arrangement of these gradiometer loops with respect to the coordinate system is indicated schematically in Fig. 8(b).

The borehole local anomaly signal, produced by flooding the crack with magnetic material, is evaluated in the previous chapter as shown by (62), and contributes to the signal at ($X = Y = 0$, $Z \approx 0$). We presume the crack producing this

anomaly signal is oriented to an arbitrary angle ϕ. We presume also that the anomaly signal, as measured by the surface magnetometer, will be sufficiently small as to be negligible. However, the total signals generated in these two gradiometers will include contributions due to the gradients of the horizontal components of the earth's field as well as gradients of noise components. The purpose of the remainder of this section is to evaluate these latter contributions and to express the total signal plus noise for each gradiometer as well as the difference signals.

In (1) $H_h = H_o(a/r)^3 \sin\theta_e$, while $\cos\theta_e$ is given by (2) in terms of μ, the geographic colatitude, λ, the geographic east longitude, and constants μ_o, λ_o. Let μ_b, λ_b denote the colatitude and east longitude, respectively, of the borehole, i.e., for any position (X = Y = 0, any value of Z), and r = a at the surface, i.e., when Z = D. Then, for any nearby position such as ($X = X_o - S\cos\chi$, $Y = S\sin\chi$, Z = D), we can evaluate the horizontal component by the Taylor's expansion,

$$H_h^{(s)} = H_o \sin\theta_b + (X - S\cos\chi)\, H_o(\partial \sin\theta/\partial\mu)_b(\partial\mu/\partial X) + S\sin\chi\, H_o\,(\partial \sin\theta/\partial\lambda)_b(\partial\lambda/\partial Y) + \ldots , \tag{85}$$

where $(\partial\mu/\partial X) = 1/a$, $(\partial\lambda/\partial Y) = 1/a$. In (85), terms of order SX/a^2, S^2/a^2, etc., are negligible.

Similarly, the H_h component at the bottom of the borehole at position ($X = S\cos\chi$, $Y = S\sin\chi$, Z = 0), i.e., the position of the center of one of the gradiometer superconducting loops, will have the form

$$H_h^{(b)} = H_o[a/(a-D)]^3 \sin\theta_b - [S\cos\chi/(a-D)]\, H_o\,[a/(a-D)]^3\,(\partial \sin\theta/\partial\mu)_b + [S\sin\chi/(a-D)]H_o\,[a/(a-D)]^3\,(\partial \sin\theta/\partial\lambda)_b + \ldots . \tag{86}$$

In the above, superscripts (s), (b), refer to surface and borehole, respectively.

Since H_h is always parallel to the X-axis, and there is never any steady part of the earth's field parallel to the Y-axis, the contribution to the gradiometer loops located at ($X - S\cos\chi$) and $S\cos\chi$, respectively, are obtained by simply

multiplying the above by $\cos\chi$. The signal in the opposite loop of each gradiometer is obtained simply by replacing S in the above expressions by - S. Subtracting this result from the above expressions then gives the gradiometer net signals except for a small correction due to the lack of exact parallelism of the gradiometer loops. The correction is discussed at some length in Ref. 9, but we shall ignore it in the present analysis. One thus finds the net contributions due to the earth's field gradients according to

$$\Delta H_h^{(s)} = -(2S/a)\, H_o\, (\partial \sin\theta/\partial\mu)_b \cos^2\chi$$

$$+(2S/a)\, H_o\, (\partial \sin\theta/\partial\lambda)_b \sin\chi\cos\chi + \text{higher order terms}, \qquad (87)$$

$$\Delta H_h^{(b)} = -(2S/a)(1 - 4D/a)\, H_o\, (\partial \sin\theta/\partial\mu)_b \cos^2\chi$$

$$-(2S/a)(1 - 4D/a)\, H_o\, (\partial \sin\theta/\partial\lambda)_b \sin\chi\cos\chi . \qquad (88)$$

Since 4D/a is of the order of (4 times one mile/4,000 miles), its contribution is only 0.001 to 0.002 of the gradiometer signal of (87). However, we will consider the effect of 4D/a on the difference signal at a later point.

The above two contributions due to the steady part of the earth's field should be the same for both the initial (i) (before flooding) and final (f) (after flooding) configurations.

The derivatives expressed in (87)-(88) are obtained directly from (2). We find

$$(\partial \sin\theta/\partial\mu)_b = -(\cos\theta/\sin\theta)(\partial\cos\theta/\partial\mu)_b ,$$

$$= -(\cos\theta_b/\sin\theta_b)\,[-\sin\mu\cos\mu_o + \cos\mu\sin\mu_o\cos(\lambda - \lambda_o)]_b \qquad (89)$$

$$(\partial \sin\theta/\partial\lambda)_b = -(\cos\theta_b/\sin\theta_b)\,[-\sin\mu\sin\mu_o\sin(\lambda - \lambda)]_b . \qquad (90)$$

The numerical values of (79) and (80) for the Jemez Mountain coordinates discussed in Sec. II. A. are 0.69380 and 0.09516, respectively.

We consider now the contributions of magnetic noise to the signals in the two gradiometers, firstly, for the case in which the noise sources are much farther away than the position coordinates ($X = X_o$, $Y = 0$, $Z = D$) and

(X = Y = 0, Z ≈ 0), from the borehole position (X = Y = 0, Z = D). The derivatives of the interfering noise signals at these points determine the magnitude of the noise components in the gradiometer signals.

We consider that the magnetic noise arising from distant sources such as lightning and/or extraterrestrial sources can be resented in vector form according to

$$\underset{\sim}{B}_N = \underset{\sim}{i}\, B_{N,x} + \underset{\sim}{j}\, B_{N,y} + \underset{\sim}{k}\, B_{N,z} \,. \tag{91}$$

The particularly noise contributions that can be represented vectorially, as in (91), can be expressed in terms of Taylor's expansions for the individual components with respect to the position (X = Y = 0, Z = D) according to

$$\begin{aligned} B_{N,p}(S\cos\chi,\ S\sin\chi,\ Z = 0) = {} & B_{N,p}(0,0,D) - S\cos\chi\ (\partial B_{N,p}/\partial X)_{00D} \\ & + S\sin\chi\ (\partial B_{N,p}/\partial Y)_{00D} \\ & - D\ (\partial B_{N,p}/\partial Z)_{00D} + \ldots \,, \end{aligned} \tag{92}$$

where p stands for the X, Y, or Z component. Similarly, the noise observed at the surface position (X = X_o - S cosχ, S sinχ, Z = D), which is at the center of one superconducting loop of the surface gradiometer, takes the form,

$$\begin{aligned} B_{N,p}(X_o - S\cos\chi,\ S\sin\chi,\ D) = {} & B_{N,p}(0,0,D) \\ & + (X_o - S\cos\chi)(\partial B_{N,p}/\partial X)_{00D} \\ & + S\sin\chi\ (\partial B_{N,p}/\partial Y)_{00D} \\ & + \text{higher order terms} \,. \end{aligned} \tag{93}$$

Again replacing S by -S in the above, we obtain the signal from the opposite gradiometer loop, which is to be subtracted from (92) and (93), respectively. Then, letting p = X, and p = Y, we obtain the components for the X-Y plane. Then multiplying the X-component by cosχ, the Y-component by sinχ and adding, we obtain the contribution parallel to the gradiometer axis which is oriented to the angle

χ. This procedure then leads to the surface and borehole noise contributions as follows:

$$\Delta B_N^{(i,s)} = -2S\,[\cos^2\chi\,(\partial B_x/\partial X) + \cos\chi\,\sin\chi\,(\partial B_y/\partial X)]^{(i)}$$

$$+ 2S\,[\sin\chi\,\cos\chi\,(\partial B_x/\partial Y) + \sin^2\chi\,(\partial B_y/\partial Y)]^{(i)}$$

$$- 2X_o S\,[\cos^2\chi\,(\partial^2 B_x/\partial X^2) + \cos\chi\,\sin\chi\,(\partial^2 B_y/\partial X^2)]^{(i)}$$

$$+ 2X_o S\,[\cos\chi\,\sin\chi\,(\partial^2 B_x/\partial X\,\partial Y) + \sin^2\chi\,(\partial^2 B_y/\partial X\,\partial Y)]^{(i)}$$

$$+ \text{other noise contributions,} \qquad (94)$$

$$\Delta B_N^{(i,b)} = -2S\,[\cos^2\chi\,(\partial B_x/\partial X) + \cos\chi\,\sin\chi\,(\partial B_y/\partial X)]^{(i)}$$

$$+ 2S\,[\cos\chi\,\sin\chi\,(\partial B_x/\partial Y) + \sin^2\chi\,(\partial B_y/\partial Y)]^{(i)}$$

$$+ 2SD\,[\cos^2\chi\,(\partial^2 B_x/\partial X\partial Y) + \cos\chi\,\sin\chi\,(\partial^2 B_y/\partial X\partial Z)]^{(i)}$$

$$- 2SD\,[\cos\chi\,\sin\chi\,(\partial^2 B_x/\partial Y\partial Z) + \sin^2\chi\,(\partial^2 B_y/\partial Y\partial Z)]^{(i)}$$

$$+ \text{other noise contributions,} \qquad (95)$$

where (i) indicates the initial state (before flooding), and the derivatives are understood to be evaluated at (0,0,D). Note that subscript N is omitted in the right-hand sides of (94) and (95).

Since several hours of time may elapse between the initial (i) measurements (before flooding) and the final (f) measurements (after flooding), we expect a considerable change in the magnitudes of the noise vector $\underset{\sim}{B}_N$, as well as in the derivatives of its components. However, the form for the (f) state will be the same as above except that superscript (i) must be changed to superscript (f).

Assuming that one can successfully subtract the borehole signal from the surface signal by some appropriate data processing method, the result will be one in which the first derivatives in the above expressions cancel in the subtraction, thereby leaving only the second derivative contributions in the difference signal

$$\Delta' B_N^{(i)} = \Delta B_N^{(i,s)} - \Delta B_N^{(i,b)}. \qquad (96)$$

Since the final configuration, after flooding, will have the same form but different magnitude, because of the time lapse factor, the noise difference signal can be expressed by

$$\Delta' B_N^{(f)} = \Delta B_N^{(f,s)} - \Delta B_N^{(f,b)}. \tag{97}$$

The total initial signal measured by the surface gradiometer at (X_o, 0, D) can then be expressed by the sum of (87) and (94). The total initial signal measured by the borehole gradiometer at (0,0,0) can be expressed by (88) plus (95). The difference between these two signals as obtained by appropriate signal processing electronics, is

$$\begin{aligned}\Delta B^{(i,s)} - \Delta B^{(i,b)} = {} & (8SD/a^2)\, H_o\, (\partial \sin\theta/\partial\mu)_b \cos^2\chi \\ & + (8SD/a^2)\, H_o\, (\partial \sin\theta/\partial\lambda)_b \cos\chi\, \sin\chi \\ & + \Delta' B_N^{(i)} + \text{electronic processing noise.}\end{aligned} \tag{98}$$

The total final signal measured by the surface gradiometer at (X_o, 0, D) is again the sum of (87) and (94), with superscripts changed to (f) in the latter. Similarly, the final signal measured by the borehole gradiometer is (88) plus (95), with superscripts changed to (f), plus now the signal due to the local anomaly as given by (62) [less than ΔB_N term in (62), which we already include in (95)]. The difference between these two final signals is then

$$\begin{aligned}\Delta B^{(f,s)} - \Delta B_N^{(f,b)} = {} & (8SD/a^2)\, H_o\, (\partial \sin\theta/\partial\mu)_b \cos^2\chi \\ & + (8SD/a^2)\, H_o\, (\partial \sin\theta/\partial\lambda)_b \cos\chi\, \sin\chi \\ & - (2\pi S \sin\psi\, m_o \Delta\phi/8)(1/r_m - 1/\rho) \\ & \times [12\cos\phi + 24\cos\chi\cos(\chi - \phi) \\ & - 45\cos\phi\cos(\chi - \phi)] \\ & + \Delta' B_N^{(f)} + \text{electronic processing noise.}\end{aligned} \tag{99}$$

As already discussed for the two-magnetometer data acquisition system of the previous section, the idea now is to record $\Delta B^{(i,s)}$, $\Delta B^{(i,b)}$, and the simultaneous difference as expressed by (98), as a function of the angle χ. Similarly, the final measurements would consist of recording $\Delta B^{(f,s)}$, $\Delta B^{(f,b)}$, and the simultaneous difference, as expressed by (99).

Assuming that the anomaly data can be acquired in the form (99), the next step in the data analysis would be to correlate the difference signal with certain functions such as

$$f_1(\chi) = \sin\chi \ ,$$

$$f_2(\chi) = \cos\chi \ ,$$

$$f_3(\chi,\phi') = \sin\chi \cos\chi \sin\phi' \ ,$$

$$f_4(\chi,\phi') = 12 \cos\phi' + 24 \cos\chi \cos(\chi - \phi') - 45 \cos\phi \cos(\chi - \phi'). \qquad (100)$$

Consider the first correlation with $f_1(\chi)$. Multiply (99) by $f_1(\chi)$ and integrate χ from 0 to 2π. This leads to

$$F_1(\phi) = -(2\pi S \sin\psi \, m_o \Delta\phi/8)(1/r_m - 1/\rho)(-45 \sin\phi \cos\phi)(2\pi/2) + \int_0^{2\pi} [\Delta' B_N^{(f)} + \text{electronic noise}] \sin\chi \, d\chi \ . \qquad (101)$$

Similarly, multiplying by $f_2(\chi)$ and integrating gives

$$F_2(\phi) = -(2\pi S \sin\psi \, m_o \Delta\phi/8)(1/r_m - 1/\rho)(-45 \cos^2\phi)(2\pi/2) + \int_0^{2\pi} [\Delta' B_N^{(f)} + \text{electronic noise}] \cos\chi \, d\chi \ . \qquad (102)$$

Note that in both of the above cases, the two leading terms of (99) integrated to zero. Thus, these particular correlations eliminate the earth's field-gradient contributions. Furthermore, if the noise contributions turn out to be random, then the last integrals of (101) and (102) will be zero. Consequently,

from the analyzed data one can calculate the ratio

$$F_1(\phi)/F_2(\phi) = \pm \tan \phi. \qquad (103)$$

In the event that F_1/F_2 should turn out to be large and unwieldy in the computer calculation, one can then calculate the ratio $F_2/F_1 = \pm \text{ctn } \phi$. The difficulty arises when ϕ is near 90° or 270°. In this case, it is desirable to correlate the experimental data with the function f_3. One obtains the result

$$F_3(\phi,\phi') = (8SD/a^2)\, H_o\, (\partial \sin\theta/\partial\lambda)_b \sin\phi' \,(2\pi/8)$$

$$- (2\pi S \sin\psi\, m_o \Delta\phi/8)(1/r_m - 1/\rho)(24 \sin\phi \sin\phi')(2\pi/8)$$

$$+ \int_o^{2\pi} [\Delta' B_N^{(f)} + \text{electronic noise}] \sin\chi \cos\chi \sin\phi' \, d\chi \,. \qquad (104)$$

Assuming the noise contribution is random, the last term again integrates to zero. One thus has a result that is dominated by the second term of (104), especially when the hydrofractured crack is filled with ferromagnetic particle slurry. A preliminary estimate of ϕ' close to true ϕ will already have been obtained by the two previous correlations. Note that the 180° ambiguity can now be resolved by replacing this starting ϕ' value by $\phi'' = \phi' + 180°$. This process completely reverses the signs of the two significant contributions of (104), assuming the noise integrates nearly to zero. Consequently, one has a practical way in which the 180° ambiguity can be resolved for the case in which the unknown ϕ is within about 10° of 90° or 270°.

Now when true ϕ lies in the range 280°-0°-80° or in the range 100°-180°-260°, the correlation of the function (99) with the function $f_4(\chi,\phi,\phi')$ will lead to the most reliable estimation of ϕ. One obtains the result

$$F_4(\phi,\phi') = (8SD/a^2)\, H_o\, (\partial \sin\theta/\partial\mu)_b (30\pi \cos\phi')$$

$$+ (8SD/a^2)\, H_o\, (\partial \sin\theta/\partial\lambda)_b\, (6\pi \sin\phi')$$

$$- (2\pi\, S \sin\psi\, m_o \Delta\phi/8)(1/r_m - 1/\rho)(9\pi)$$

$$X\ [144\ \cos\phi\ \cos\phi' + 225\ (\cos^2\phi\ \cos^2\phi' + \sin\phi\ \cos\phi\ \sin\phi'\ \cos\phi')]$$

$$+ \int_0^{2\pi} [\Delta' B_N^{(f)} + \text{electronic noise}]\ f_x(\chi,\phi,\phi')\ d\chi\ . \qquad (105)$$

The two leading earth's field terms in (105) are very small compared to the anomaly term, and the latter is further enhanced by the correlation process. Meanwhile, the noise term again is negligible if the noise is random. Thus, the anomaly part of (105) is by far the dominant part of the correlation function F_4. However, the 180° ambiguity will still be present in the correlation with the actual experimental difference signal. This ambiguity can be resolved, as before, by again correlating with the function $f_4(\chi,\phi,\phi'')$, where $\phi'' = \phi' + 180°$. Thus, with ϕ'' in place of ϕ' in (105) the effect will be to change the sign of the two leading terms, while the square bracket in the anomaly term becomes

$$-144\ \cos\phi\ \cos\phi'' + 225(\cos^2\phi\ \cos^2\phi'' + \sin\phi\ \sin\phi''\ \cos\phi\ \cos\phi'')\ . \qquad (106)$$

Thus, if ϕ' is initially a good estimate of ϕ, then the correlation with ϕ'' will lead to a significantly smaller value for the function F_4. On the other hand, if the initial choice ϕ' is off by 180°, then the use of ϕ'' will give a larger value for the function F_4. Thus, by this process, we can resolve the 180° ambiguity, when ϕ is in the ranges discussed just above.

An example of gradiometer signal strengths can be based on the same parameters used for the magnetometer case in the previous section [see discussion preceding (74)]. The hydrofractured crack has an assumed radius of 100 m and a width of 2 mm. For the equivalent wedge volume, $\Delta\phi = 1.5 \times 10^{-5}$ radians, $\rho = 100$ m. The gradiometer factor

$$f_g = (2\pi S\ \sin\psi\ m_o \Delta\phi/8), \qquad (107)$$

with $S = 2$ cm, m_o as above [see (74)], is then

$$f_g = 7.5 \times 10^{-10}\ \text{Oe-cm (paramagnetic solution)},$$

$$f_g = 1.0 \times 10^{-4}\ \text{Oe-cm (prepolarized ferromagnetic 1\% particle slurry)}. \qquad (108)$$

The earth's steady horizontal component gradient factors, for an assumed borehole depth of one mile, are

$$(2S/a)\ H_o\ (\partial \sin\theta/\partial\mu)_b = 0.66 \times 10^{-9}\ \text{Oe},$$

$$(2S/a)\ H_o\ (\partial \sin\theta/\partial\lambda)_b = 0.90 \times 10^{-10}\ \text{Oe},$$

$$(2SD/a^2)\ H_o\ (\partial \sin\theta/\partial\mu)_b = 0.7 \times 10^{-12}\ \text{Oe},$$

$$(2SD/a^2)\ H_o\ (\partial \sin\theta/\partial\lambda)_b = 0.9 \times 10^{-13}\ \text{Oe}. \qquad (109)$$

The borehole gradiometer signal, by itself, is the combination of (58)-(62) less the ΔB_N term in (62), plus (88), plus (95), with superscript changed from (i,b) to (f,b), plus small gradiometer imperfection terms as described below. We express this combination in the form

$$\begin{aligned}\Delta B_g^{(f,b)} = &- \Big\{(2\pi S \sin\psi\ m_o\Delta\phi/8)(1/r_m - 1/\rho)\ [12\cos\phi \\ &+ 24\cos\chi\cos(\chi-\phi) - 45\cos\phi\cos(\chi-\phi)]\Big\} \\ &- [(2S/a)\ H_o\ (\partial\sin\theta/\partial\mu)_b\cos^2\chi \\ &+ (2S/a)\ H_o\ (\partial\sin\theta/\partial\lambda)_b\cos\chi\sin\chi\ ] \\ &+ \Delta B_N^{(f,b)} + h\Big\{H_o\sin\theta_b\cos\chi + m_o\Delta\phi\sin\psi\log(\rho/r_m) \\ &X[4\cos\phi\cos(\chi-\phi) - 2\cos\chi]\Big\} \\ &+ h(B_{N,x}\cos\chi + B_{N,y}\sin\chi)\ , \end{aligned} \qquad (110)$$

in which h is a small numerical factor, of the order of 10^{-5} to 10^{-7}, that represents the imperfection of the gradiometer. It comes about because the two superconducting loops of the gradiometer may not be exactly parallel, or because one loop may have a slightly larger area than the other. There are a number of tricks in the business whereby the factor h can be reduced by fine adjustments to the above magnitude. The product of h with the gradient parts of the magnetometer signal, and parts containing $\Delta\phi$, is negligibly small, i.e., of the order of

10^{-10} to 10^{-14} Oe. However, the steady part of the component H_h and the x- and y-components of the noise mix into the gradiometer signal as significant magnetometer components. We shall evaluate each component of (110) for the set of parameters given above. The leading term in curly brackets, which we denote by $\{A\}$, is the local anomaly contribution. When r_m = 2 m, the value discussed in Sec. V. A.), one finds

$$\{A\} = \left\{(3.75 \times 10^{-12} \text{ Oe}) \times f(\chi,\phi)\right\}; \text{ (paramagnetic solution)},$$
$$= \left\{(0.5 \times 10^{-6} \text{ Oe}) \times f(\chi,\phi)\right\}; \text{ (ferromagnetic slurry)}, \qquad (111)$$

where $f(\chi,\phi)$, as given by (63), has a maximum peak absolute value of 81, and a minimum peak absolute value of 12. Thus, the peak signal range of $\{A\}$ is 3.0×10^{-10} and 0.45×10^{-10} Oe; (paramagnetic solution), and 4.0×10^{-5} and 6.0×10^{-6} Oe; (ferromagnetic slurry), respectively. This result is to be compared with the second term of (110) in square brackets, which represents the gradient of H_h, and has the magnitude

$$[\nabla H_h] = [0.66 \cos^2\chi + 0.09 \sin\chi \cos\chi] \times 10^{-9} \text{ Oe}. \qquad (112)$$

The noise gradient term $\Delta B_N^{(f,b)}$ is not expected to exceed $[\nabla H_h]$, and generally is expected to be much smaller. Moreover, it is expected to be random when averaged over a suitable time scale.

The last two terms of (110) are troublesome. For an imperfection factor in the range $10^{-7} < h < 10^{-5}$,

$$2.1 \times 10^{-8} \text{ Oe} < h H_o \sin\theta_b < 2.1 \times 10^{-6} \text{ Oe}, \qquad (113)$$

which exceeds $\{A\}$ by 2 to 5 orders in the paramagnetic solution case, and is comparable to $\{A\}$ in the ferromagnetic slurry case. However, correlation with the function $f_1(\chi)$ and $f_3(\chi,\phi')$, eliminates this troublesome contribution. Another way to obtain a minimal contribution from this source is to subtract the borehole signal from the surface signal, as discussed above. If the two gradiometers have similar imperfection factors, then the magnetometer-type contributions will nearly cancel.

Experimental observation on the diurnal variation of H_h, which we consider to be noise, shows maximum excursions of 100 gamma for long periods of several hours but only of the order of 10 gamma or less for the short periods needed to complete the borehole gradiometer signal acquisition. Thus the noise imperfection contribution to (110) is expected to be in the range

$$10^{-11} \text{ Oe} < h \times \text{noise} < 10^{-9} \text{ Oe}, \tag{114}$$

which is greater than the $\{A\}$ contribution for the paramagnetic solution case but significantly smaller than $\{A\}$ for the ferromagnetic slurry case.

The above analysis therefore proves that using either the borehole gradiometer by itself, or by combining signals from the borehole and surface gradiometers, that the angle ϕ of the crack produced by hydrofracturing can be determined. The cross-correlation of the data, as described above, must be used in this determination in order to eliminate the 180° ambiguity, as discussed earlier. We conclude also that the use of a paramagnetic solution in the crack does not give a large enough magnetic moment in order to distinguish the magnetic anomaly in the presence of interfering noise and imperfection signals. However, the use of only 1% of ferromagnetic prepolarized particles in a slurry pumped into the crack, produces an anomaly signal that is larger than the interfering signals, so that the anomaly orientation can be readily determined.

The above analysis is based on a conservative choice of a crack produced by hydrofracturing that is only 2 mm wide and 100 m radius.

VI. ANOMALY DETECTION BY SURFACE GRADIOMETERS

A. Signals Due to Spherical Distributions

The superconducting gradiometer signal due to deep spherical distributions of magnetic material of radius ρ can be calculated directly from the results (30)-(33). One simply selects the appropriate Taylor's expansion for a given gradiometer configuration and combines the results for the two loops.

For example, consider an axial-type gradiometer the center of which is located at a point on the surface at (X_o, Y_o, D), with its axis in the X-Y plane, and rotated to an arbitrary angle χ. One loop of the gradiometer will have its center at the point $(X_o + S\cos\chi, Y_o + S\sin\chi, D)$. The expansions of (30) and (31) for this case are, respectively,

$$B_x = B_x(X_o,Y_o,D) + S\cos\chi\ (\partial B_x/\partial x)_{X_o,Y_o} + S\sin\chi\ (\partial B_x/\partial y)_{X_o,Y_o}\ , \qquad (115)$$

$$B_y = B_y(X_o,Y_o,D) + S\cos\chi\ (\partial B_y/\partial x)_{X_o,Y_o} + S\sin\chi\ (\partial B_y/\partial y)_{X_o,Y_o}\ . \qquad (116)$$

The magnitude of the field vector at $(X_o + S\cos\chi,\ Y_o + S\sin\chi, D)$ in the direction χ is then $B_x\cos\chi + B_y\sin\chi$. The magnitude of the field at the center of the opposite gradiometer loop at $(X_o - S\cos\chi,\ Y_o - S\sin\chi, D)$ is obtained by substituting -S in the place of S in (115)-(116). The gradiometer signal, which is proportional to the difference of these two expressions, is then given by

$$\Delta B(\chi) = 2S\Big\{\cos^2\chi\ (\partial B_x/\partial x) + \sin\chi\cos\chi\ [(\partial B_x/\partial y) + (\partial B_y/\partial\chi)] + \sin^2\chi\ (\partial B_y/\partial y)\Big\}$$
$$+\Delta H_h^{(s)} + h\,H_o\sin\theta_b\cos\chi + \text{noise}\ . \qquad (117)$$

The derivatives in (117) are understood to be evaluated at (X_o,Y_o,D), $\Delta H_h^{(s)}$ is the earth's field horizontal gradient contribution as in (87), , and the next to last term is the magnetometer component in the gradiometer signal due to gradiometer imperfection. As pointed out at (110), the imperfection factor h can be made as small as 10^{-5} to 10^{-7}.

The derivatives of (30) and (31) are

$$(\partial B_x/\partial x)_{X_o,Y_o} = -(5X_o/R_o^2)B_x(X_o,Y_o) + (4\pi m_o\rho^3/3R_o^5)(4X_o\sin\psi + 3D\cos\psi), \qquad (118)$$

$$(\partial B_x/\partial y)_{X_o,Y_o} = -(5Y_o/R_o^2)B_x(X_o,Y_o) + (4\pi m_o\rho^3/3R_o^5)(-2\,Y_o\sin\psi)\ , \qquad (119)$$

$$(\partial B_y/\partial x)_{X_o,Y_o} = -(5X_o/R_o^2)B_x(X_o,Y_o) + (4\pi m_o\rho^3/3R_o^5)(3\,Y_o\sin\psi)\ , \qquad (120)$$

$$(\partial B_y/\partial y)_{X_o,Y_o} = -(5Y_o/R_o^2)B_x(X_o,Y_o) + (4\pi m_o\rho^3/3R_o^5)(3X_o\sin\psi + 3D\cos\psi). \qquad (121)$$

Substituting (118)-(121) into (117) then gives the desired gradiometer contribution from the anomaly, for the gradiometer axis in the X-Y plane, plus the additional small contributions. The anomaly part of (117) is evaluated for several positions (X_o, Y_o, D) and several orientation angles, χ's, in Table 3. In addition, the gradiometer anomaly signal contribution is evaluated in Table 3 for the case in which the gradiometer axis is vertical, i.e., parallel to Z. This contribution is obtained by differentiating (32) with respect to Z (or D).

TABLE 3

AXIAL SUPERCONDUCTING GRADIOMETER FUNCTIONS FOR SEVERAL GRADIOMETER POSITIONS ON THE SURFACE AND FOR SEVERAL ORIENTATIONS OF THE GRADIOMETER AXIS

Position	Axis Orientation	Fig. 8	Formula: $(4\pi F m_o r_m^3/R^3)$ (2s/R) X Function Below	Function Value X,Y/D=1/4,1/3,1/2
X=0,Y,D	$\|\|X;\chi=0$	(b)A	$3D\cos\psi/R$	0.670 0.893 1.339
X=0,Y,D	$\|\|Y;\chi=90°$	(b)A	$3D(D^2-4Y^2)\cos\psi/R^3$	1.834 1.270 0.0
X=0,Y,D	$\|\|Z$	(a)A	$-D(6D^2-9Y^2)\cos\psi/R^3$	4.432 3.811 2.395
X,Y=0,D	$\|\|X;\chi=0$	(b)A	$[D(3D^2-12X^2)\cos\psi$ $+X(9D^2-6X^2)\sin\psi]/R^3$	2.721 2.339 1.209
X,Y=0,D	$\|\|Y;\chi=90°$	(b)A	$3(D\cos\psi + X\sin\psi)/R^3$	2.754 2.671 2.400
X,Y=0,D	$\|\|Z$	(a)A	$-[D(6D^2-9X^2)\cos\psi$ $+X(12D^2-3X^2)\sin\psi]/R^3$	5.647 5.307 4.209
X=Y,D	+45° from X in XY plane	(b)A	$2[D(D^2-8X^2)\cos\psi$ $+X(3D^2-4X^2)\sin\psi]/R^3$	1.374 0.824 -0.956
X=Y,D	-45° from X in XY plane	(b)A	$X(6D^2+12X^2)\sin\psi/R^3$	0.694 0.941 1.451
X=Y,D	$\|\|Z$	(a)A	$-[D(6D^2-18X^2)\cos\psi$ $+X(12D^2-6X^2)\sin\psi]/R^3$	5.17 4.50 2.69

The last column in Table 3 shows the relative strength of the anomaly signal in terms of position for various locations on the surface such as $X_o/D = 1/4$, 1/3, and 1/2 and/or $Y_o/D = 1/4$, 1/3, and 1/2. These values indicate that there is some position at which the gradiometer signal strength will be a maximum. This position can be found by differentiation. It is also shown in Table 3 that the signal always will be greatest when the gradiometer axis is vertical, rather than in the X-Y plane.

We consider the following example of an anomaly produced by a spherical distribution of magnetic material: a 1% slurry of ferromagnetic particles occupies a spherical volume of radius ρ, where ρ is determined for a sphere having the same volume as a hydrofractured crack of 2.0-mm width and 300-m radius. For this assumption, we find the equivalent ρ of 4.1 m. We consider now the magnetic moment parameters as discussed near (74), for a sphere located at a depth of one mile. A vertically oriented gradiometer located at (X_o, Y=0, Z=D) will then pick up an anomaly signal component of strength

$$\Delta B_z = (4\pi m_o \rho^3/R^3)(2S/R)\ [(6D^3 - X_o^2 D)\cos\psi + (12X_o D^2 - 9X_o^3)\sin\psi\ ]/R^3\ , \qquad (122)$$

as given in Table 3. When $X_o = 1/4D$ (note function value of 5.647 column of Table 3), we thus find the gradiometer anomaly signal component will have the amplitude

$$\Delta B_z = 0.9 \times 10^{-10}\,\text{Oe}\ . \qquad (123)$$

At the same time, the gradiometer will also have a component due to the gradient of the vertical component of the earth's field. Using (1) we find this component will have the magnitude $(2S/a)H_r$, where $H_r = 0.436$ Oe, and $a = 6.37 \times 10^8$ cm. This component is then about 1.3×10^{-9} Oe, or some 15 times greater than the above ΔB_z. To distinguish a signal this small, which is just comparable to 30-MHz SQUID sensitivity, out of a background of 1.3×10^{-9} Oe, it will be necessary to measure before producing the anomaly, remeasure after producing the anomaly, and then determine the difference. Long-time averaging of signals will be necessary both before and after producing the anomaly.

There are two ways to improve matters. The first is to use a gradiometer spacing 2S of 20 cm rather than using the 2.0 cm in the example (123). While this will increase ΔB by a factor of ten, it will simultaneously increase the earth's field vertical component gradient contribution by the same factor.

Another way is to increase the magnetic material in the slurry from a 1% slurry to, say a 10% slurry. If both of these things are done, then the ΔB component can be increased to something like 100 times the 10^{-10} 0e basic sensitivity of the 30-MHz SQUID, for the assumed spherical distribution of radius $\rho = 4.0$ m. Thus, one should be able to determine the relative size of the anomaly, i.e., the value of ρ, but such a signal will not contain any directional information.

We consider now a second example, i.e., the anomaly produced by a geological coal or oil deposit, which is diamagnetic with respect to the surrounding underburden and overburden rocks. Such deposits are often found in lens-shaped sandbars. The sand material of a typical sand lens has a susceptibility of 2.5×10^{-6} cgs, while invasion by oil (susceptibility = -0.8) will reduce this to something like 2.0×10^{-6} cgs. If surrounded by a typical shale (susceptibility of 20 to 25×10^{-6} cgs), the discontinuity in susceptibility will be the factor that produces a local diamagnetic dipole with effective susceptibility of around 20×10^{-6} cgs. Thus each cm^3 of material will exhibit an effective moment $m_o = 10 \times 10^{-6}$ 0e, since the material is polarized by an earth's field of magnitude 0.5 0e. Assuming a gradiometer spacing of 20 cm and a region with an effective spherical radius of 300 m at a depth of one mile, and an assumed location ($X_o = 1/4D$, $Y_o = 0$, $Z_o = D$), we find the gradiometer signal strength to be

$$\Delta B_Z = 2.3 \times 10^{-10} \text{ 0e} + \Delta H_r + hH_r + \text{noise} , \qquad (124)$$

where $\Delta H_r = 1.3 \times 10^{-8}$ 0e (for gradiometer with 20-cm loop spacing) and will be constant for all positions close to the anomaly, while gradiometer imperfection factor h should again be in the range 10^{-7} to 10^{-5}, and the imperfection term will again be constant. Notice in Table 3 that as surface position is changed, the gradiometer contribution changes significantly, as indicated by the numbers in the function value column. Thus, movement of the gradiometer to different positions while comparing the signal, and while maintaining ΔH_r and hH_r fixed, will indicate the presence and approximate location of the anomaly. This is accomplished most efficiently by putting the gradiometer on an airborne platform. Note that the factor 2.3×10^{-10} is only a little larger than the sensitivity of a 30-MHz SQUID. However, by the use of a superconducting flux transformer arrangement, the signal at the SQUID sensor itself can be increased by a factor of 20 to 50 times this basic sensitivity.

B. Signals Due to Wedge Distributions

Consider an axial gradiometer located on the surface at a point (X_o, Y_o, D), as in Fig. 4, with its axis oriented to an angle χ in the X-Y plane. The signal response to a wedge anomaly oriented to any angle ϕ is given by (117) when the appropriate derivatives are used. In this case, the expressions to be differentiated are (40) and (41). For convenience, we choose the case in which the gradiometer is located on the isogonic line Y = 0, and obtain

$$(\partial B_x/\partial X)_{Y=0} = (2\, m_o \Delta\phi \rho^3/3R^4)(3d^3\cos\psi - 12x^2 d\cos\psi - 6x^3\sin\psi + 9xd^2\sin\psi)$$
$$+ (m_o \Delta\phi \rho^4/8R^5)(\cos\phi)(81x^2\sin\psi + 45xd\cos\psi - 9d^2\sin\psi$$
$$- 105\, x^3 d\cos\psi - 105\, x^4 \sin\psi)\ , \qquad (125)$$

$$(\partial B_x/\partial Y)_{Y=0} = (m_o \Delta\phi \rho^4/8R^5)(\sin\phi)(-3d^2\sin\psi + 15\, xd\cos\psi + 12x^2\sin\psi)$$
$$= (\partial B_y/\partial X)_{Y=0}\ , \qquad (126)$$

$$(\partial B_y/\partial Y)_{Y=0} = (2\, m_o \Delta\phi \rho^3/3R^4)(d\cos\psi + x\sin\psi)$$
$$+ (m_o \Delta\phi \rho^4/8R^5)(\cos\phi)(-3d^2\sin\psi + 15xd\cos\psi + 12x^2\sin\psi)\ , \qquad (127)$$

where $d = D_o/R_o$, $x = X_o/R_o$, $R_o = (X_o^2 + D_o^2)^{1/2} = R$ (above), and the derivatives are evaluated at $(X=X_o,\ Y=Y_o=0,\ Z=D_o)$.

When the above results are substituted into (117) one sees the possibility of determining the angular orientation ϕ of the wedge distribution in the terms that are of the order (ρ/R) smaller than the leading terms.

We can get an indication of the expected magnitudes of the above contributions by assuming $(X_o = 1/4\, D_o,\ Y_o=0,\ D)$ for the gradiometer location. For this point, the above derivatives have the values

$$(\partial B_x/\partial X) = (m_o \Delta\phi/R)\,[(1.150)(\rho^3/R^3) + (0.695\cos\phi)(\rho^4/R^4)]\ , \qquad (128)$$

$$(\partial B_x/\partial Y) = (\partial B_y/\partial X) = (m_o \Delta\phi/R)(0.101\sin\phi)(\rho^4/R^4)\ , \qquad (129)$$

$$(\partial B_y/\partial Y) = (m_o \Delta\phi/R)\,[(0.599)(\rho^3/R^3) + (0.101\cos\phi)(\rho^4/R^4)]\ . \qquad (130)$$

The contributions to the expected signal produced by the horizontal axial gradiometer can be written down in terms of the above derivatives, (117), and the earth's field contribution expressed by (87), in the form

$$\Delta B_g(\chi) = (2S/R)(m_o \Delta\phi) \left\{(\rho^3/R^3)(1.15 \cos^2\chi + 0.6 \sin^2\chi)\right.$$
$$+ (\rho^4/R^4)[\cos\phi\ (0.695 \cos^2\chi + 0.101 \sin^2\chi)$$
$$\left. + \sin\phi\ (0.202)\ \sin\chi\ \cos\chi]\right\}$$
$$+ (2S/a)\ H_o[(\partial \sin\theta/\partial\mu)\cos^2\chi + (\partial \sin\theta/\partial\lambda)\ \sin\chi\ \cos\chi]$$
$$+ h\ H_o\ \sin\theta\ \cos\chi + \text{noise} . \qquad (131)$$

If we now assume 2S = 20 cm, and, as in previous examples, D = one mile, ρ = 300 m, $\Delta\phi = 1.5 \times 10^{-5}$ radians, m_o = 9.5 Oe (for a 1% slurry of ferromagnetic material), we obtain the relative contributions

$$\Delta B_g(\chi) = \left\{(1.8 \times 10^{-10})\cos^2\chi + (1.3 \times 10^{-10})\sin^2\chi\right.$$
$$+ \cos\phi\ [1.4 \times 10^{-11})\cos^2\chi + (1.0 \times 10^{-11})\sin^2\chi]$$
$$\left. + \sin\phi\ (1.0 \times 10^{-11})\sin\chi\ \cos\chi\right\}$$
$$+ [66.0 \times 10^{-10}\cos^2\chi + 9.0 \times 10^{-10}\sin\chi\ \cos\chi]$$
$$+ h(0.3)\cos\chi + \text{noise} . \qquad (132)$$

The anomaly contribution to the signal (within the curly brackets) contains terms having a (ρ^4/R^4) dependence that are multiplied by the $\cos\phi$ and $\sin\phi$ and should, in principle, permit the determination of ϕ. Unfortunately, these terms are always an order (ρ/R) smaller than the leading terms. It may be that it is not possible to extract these terms out of the total signal by cross-correlation analysis. We discuss later possible ways of increasing the overall anomaly signal amplitude as well as some possible means of analyzing the data.

One of the main objections to the use of the horizontal axial gradiometer is that the imperfection contribution may be 10^2 to 10^4 larger than the anomaly con-

tribution. Moreover, this contribution is modulated by $\cos\chi$ and, because it is so relatively large, it becomes difficult to eliminate via cross-correlation analysis. We have already discussed one way to cancel out such contributions. In the present case, this would involve using a second horizontal axial gradiometer at a position where the anomaly contribution is negligible but where the earth's field gradient and imperfection contributions are essentially the same. Subtraction of these two contributions would reduce their effect to the point that cross-correlation analysis could be used on the difference signal to define mainly the anomaly contribution. Another point is that, if the anomaly contribution could be increased by a factor of 10 to 100, it should be possible to use the function $\sin\chi\cos\chi$ in cross-correlation analysis to define the $\sin\phi$ term. One way to increase the anomaly contribution would be to increase the volume of ferromagnetic particles in slurry from the 1% assumed in all of the above calculations to 10%. As already mentioned, a second way would be to use a one-to-ten flux transformer in conjunction with the gradiometer.

Another method for the study of the anomaly produced by filling the hydrofractured crack would be to use a planar gradiometer system such as that shown in Fig. 8 (c). We shall see below that this system has certain advantages over the axial gradiometer system. The planar gradiometer signal is derived from the Taylor's expansion of (42) for a position $(X_o + S\cos\chi,\ Y_o + S\sin\chi,\ Z_o=D)$ with respect to the position (X_o, Y_o, D). We consider the case in which the axis of the plane of the gradiometer is always in the X-Y plane of the figure and the axis of rotation is parallel to Z and about the gradiometer center line. In this case the signal is given by

$$\Delta B_p = (m_o \Delta\phi \rho^3/R^3)(2S/R)\ [2d\cos\chi\sin\psi + 2(x\cos\chi + y\sin\chi)\cos\psi$$

$$-10\,d\,(x\cos\chi + y\sin\chi)(d\cos\psi + x\sin\psi)]$$

$$+ (m_o \Delta\phi \rho^4/R^4)(2S/R)\ \{-(3/8)\cos\psi\cos(\chi - \phi)$$

$$+ (15\,d/8)\ [(x\cos\chi + y\sin\chi)(d\sin\psi\cos\phi + (x\cos\phi + y\sin\phi)\cos\psi)$$

$$+ (d\cos\psi + x\sin\psi)\cos(\chi - \phi) + \cos\chi\sin\psi\ (x\cos\phi + y\sin\phi)]$$

$$- (75d/8)\ [\cos\phi\ (d\cos\psi + x\sin\psi)(x\cos\phi + y\sin\phi)(x\cos\chi + y\sin\chi)]\}$$

$$+ (2S\cos\chi/a)(2H_o)(\partial\cos\theta/\partial\mu) + (2S\sin\chi/a)(2H_o)(\partial\cos\theta/\partial\lambda)$$

$$+ 2hH_o\cos\theta + O(hS/a)\cos\chi + O(hS/a)\sin\chi + \text{noise}. \qquad (133)$$

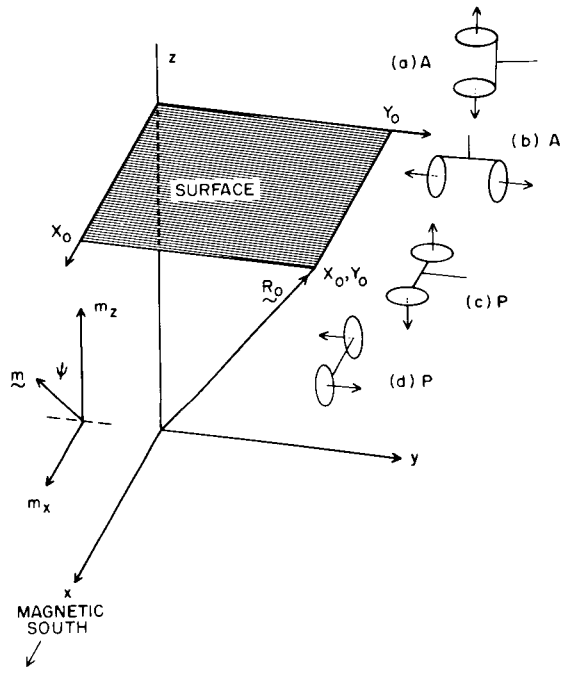

Fig. 8.
Some of the possible configurations of superconducting gradiometers: (a) A, axial-type, axis vertical; (b) A, axial-type, axis in the x-y plane, can be rotated to any azimuthal angle χ; (c) P, planar-type, measures z-component of magnetic fields, can be rotated to any azimuthal angle χ; (d) P, planar-type, measures combination of X and Y components of fields, can be rotated to any azimuthal angle χ.

In this result, only the vertical component of the earth's field appears and it is multiplied by the imperfection factor h, which makes its contribution of the order of 3×10^{-6} to 3×10^{-8} 0e. Unlike Eqs. (131-132), this term is not modulated by the rotation angle χ, as in the previous case of the axial gradiometer, except in the two second-order contributions, $O(hS/a)\cos\chi$ and $O(hS/a)\sin\chi$, which contribute negligible amounts of around 10^{-14} 0e. It therefore contributes only a constant amount as the gradiometer is rotated. The vertical component gradient contributions are about $130 \times 10^{-10}\cos\chi$ 0e and $18 \times 10^{-10}\sin\chi$ 0e, respectively, when we assume 2S = 20 cm as in the previous example; these are the fifth and sixth from last terms of (133).

To compare the planar and axial gradiometer signals, we shall use the same parameters as in (132), i.e., $X_o = 1/4\ D$, $Y_o = 0$, $Z_o = D$ in (133). We obtain

$$\Delta B_p = \left\{(1.00 \times 10^{-10})\cos\chi + [0.089 \times 10^{-10}\cos\chi\cos\phi\right.$$

$$\left. + 0.32 \times 10^{-10}\cos(\chi - \phi) - 0.097 \times 10^{-10}\cos\chi\cos^2\phi]\right\}$$

$$- [133 \times 10^{-10}\cos\chi + 18 \times 10^{-10}\sin\chi]$$

$$+ h(0.436) + \text{magnetic noise}. \qquad (134)$$

The hydrofractured crack anomaly signal, as seen by the planar gradiometer at $(X_g,0,D)$, is contained in the curly brackets of (134). The part with the (ρ^4/R^4) dependence is within the square brackets in the curly brackets. As with the axial gradiometer, these contributions are about an order of magnitude smaller than the leading anomaly contribution but could contain the possibility of defining the angle ϕ of the crack orientation.

The advantage of this particular planar gradiometer arrangement is that the large imperfection contribution is essentially a constant so that the earth's field-gradient contributions plus the anomaly contribution rides on top of it. The fact that the earth's field-gradient contribution is large compared to the anomaly contribution is not much more of a disadvantage for the planar than for the axial gradiometer. Again, the best way to eliminate this is to subtract it, either from the signal obtained prior to producing the anomaly, or from the synchronized signal produced by a second nearly identical gradiometer in which the anomaly contribution is negligible.

It is beyond the scope of the present work to analyze the signals possible in some 12 axial and planar gradiometer configurations. Nevertheless, it is almost certain that some combinations of two gradiometers can essentially completely eliminate the undesirable signals while enhancing the desired anomaly contribution. With some of these it should be possible to obtain a reliable definition of the orientation ϕ of the hydrofractured crack.

C. Signals Due to Crack Distributions

The gradiometer signals for the crack distribution can be calculated by differentiating (44), (45), and (46) and then by using appropriate combinations of these with the factor 2S, the gradiometer loop spacing. The procedure is to replace fixed X_o by variable X, Y_o by Y, D by Z, and differentiate with respect to these variables. We consider first the signals produced in an axial gradiometer with vertical orientation. In this case we need only the derivative $(\partial B_z/\partial Z)$ times the factor 2S. For this gradiometer the signal contribution from the crack anomaly is then

$$\Delta B_g = (\pi m_o t\rho^2/R^3)(2S/R)\ [3(X_o \sin\psi + 2D\cos\psi)/R$$

$$-15\ D^2(X_o\sin\psi + D\cos\psi)/R^3]$$

$$+ (2m_o t\rho^3/3R^4)(2S/R)\ [-3\cos\phi\sin\psi$$

$$+ 15D(X_o\cos\phi\cos\psi + Y_o\sin\phi\cos\psi + D\cos\phi\sin\psi)/R^2$$

$$+ 15(X_o\sin\psi + 2D\cos\psi)(X_o\cos\phi + Y_o\sin\phi)/R^2$$

$$- 105\,D^2(X_o\sin\psi + D\cos\psi)(X_o\cos\phi + Y_o\sin\phi)/R^4]\ . \qquad (135)$$

We shall evaluate this signal contribution for the point $X_o = D/4$, $Y_o = 0$, $Z_o = D$ for the case in which the anomaly is filled with the 1.0% ferromagnetic slurry, i.e., m_o has the value used in (74), the crack is 0.2 cm wide and has the radius 300 m, the borehole is one mile deep (1609 m), and 2S = 20 cm. For these assumed parameters we obtain at the surface an anomaly **contribution**

$$\Delta B_g = 6.6 \times 10^{-10} + 0.99 \times 10^{-10}\cos\phi\ \mathbf{0e}\ , \qquad (136)$$

assuming a one-to-one relationship between the gradiometer signal and the field change at the point in the shield where the SQUID is located. As in all previous calculations, we have not used transformer step up to increase the field at the SQUID itself, although this option is always open in the practical design of a system.

In the comparison of this result for the actual crack distribution with the corresponding result for the wedge distribution as given by (123), we find the steady part of the signal is seven times greater for the actual crack than that calculated for the wedge, while the part of (136) expressing the $\cos\phi$ dependence is the same magnitude as B_z for the wedge. This interesting result shows further that our calculations for the wedge distribution are on the conservative side.

The next important case is that of the signal produced by the crack distribution in a horizontal gradiometer rotated to the angle χ. We will consider the position ($X = X_o$, $Y = 0$, $Z = D$), for which the appropriate derivatives of (44) and (45) are

$$(\partial B_x/\partial X) = (\pi m_o t\rho^2/2R^4)\ [(9x\sin\psi + 3d\cos\psi) - 15\ (x^3\sin\psi + x^2 d\cos\psi)]$$

$$+ (2m_o t\rho^3/3R^5)\ [-9\cos\phi\sin\psi + 15(6x^2\sin\psi + 3xd\cos\psi)\cos\phi$$

$$- 105\ (x^4 \sin\psi + x^3 d \cos\psi)\cos\phi]\ , \tag{137}$$

$$(\partial B_x/\partial Y) = (2\ m_o t\rho^3/3R^5)\ [-3 \sin\phi \sin\psi + 15\ (x^2\sin\psi + xd \cos\psi)\cos\phi]\ , \tag{138}$$

$$(\partial B_y/\partial Y) = (\pi m_o t\rho^2/2R^4)\ [(x \sin\psi + d \cos\psi)]$$

$$+ (2\ m_o t\rho^3/3R^5)\ [-3 \cos\phi \sin\psi + 15(x^2 \sin\psi + xd \cos\psi)\cos\phi], \tag{139}$$

in which $x = X_o/R$, $d = D/R$, $R^2 = X_o^2 + D^2$, and $(\partial B_x/\partial Y) = (\partial B_y/\partial X)$. The above results were obtained by first replacing constants X_o and Y_o in (44) and (45) by X and Y and then carrying out the indicated differentiation. The gradiometer signal becomes a function of rotation angle χ when the above derivatives are substituted into (117). The relative magnitudes of the anomaly and earth's field gradient contributions will be about the same as in (132) for the wedge distribution.

We now propose a method for subtracting out the large, earth's field-gradient contribution. We will use two gradiometers, one located at $(X_o,0,D)$ and the second at $(-X_o,0,D)$ on the opposite side of the borehole. In the data analysis system, we will subtract these two signals, and then perform computer correlation analyses on the difference signal. The difference signal is given by

$$(\text{diff.}\Delta B) = (4S/R)(\pi m_o t\rho^2/2R^3)\ [\cos^2\chi\ (9x - 15x^3)\ \sin\psi + 3\ x\ \sin\psi\ \sin^2\chi]$$

$$+ (4S/R)(2m_o t\rho^3/3R^4)\ [\cos^2\chi\ \cos\phi\ \cos\psi\ (45\ xd - 105\ x^3 d)$$

$$+ 2\ \cos\chi\ \sin\chi\ \cos\psi\ \sin\phi\ (15\ xd)$$

$$+ \sin^2\chi\ \cos\psi\ \cos\phi\ (15\ xd)] + \Delta H_{imp}\ \cos\chi + \text{noise}\ . \tag{140}$$

Notice in (132) that subtraction would cancel the earth's field gradient components but would not cancel the imperfection contributions since h of the gradiometer at $+ X_o$ could not be expected to be the same as h at $- X_o$. The difference in these two signals, shown as ΔH_{imp} in (140), will disappear on computer correlations with the functions $\cos^2\chi$, or $\sin^2\chi$, or $\cos\chi\ \sin\chi$, because it varies as $\cos\chi$. These correlations, equivalent to the following integrations, are given by

$$\int(\text{diff.}\Delta B)\cos^2\chi d\chi = (4S/R)(\pi m_o t\rho^2/R^3)\left\{[(3\pi/4)(x)(9-15x^2) + (\pi/4)(3x)]\sin\psi\right.$$

$$\left. + (4\rho/3\pi R)\,[(3\pi/4)(45 - 105\,x^2)xd + (\pi/4)(15xd)]\cos\psi\cos\phi\right\}, \qquad (141)$$

$$\int(\text{diff.}\Delta B)\sin^2\chi d\chi = (4S/R)(\pi m_o t\rho^2/R^3)\left\{[(\pi/4)(x)(9-15x^2) + (3\pi/4)(3x)]\sin\psi\right.$$

$$\left. + (4\rho/3\pi R)\,[(\pi/4)(45 - 105\,x^2)xd + (3\pi/4)(15xd)]\cos\psi\cos\phi\right\}, \qquad (142)$$

$$\int(\text{diff.}\Delta B)\sin\chi\cos\chi\, d\chi = (4S/R)(\pi m_o t\rho^2/R^3)(4\rho/3\pi R)(2\pi/4)(15xd)\cos\psi\sin\phi. \qquad (143)$$

These integrations should be carried out over several complete cycles of the angle χ so that the noise contribution will have a better chance of integrating out to zero. If we now take the ratios of these computed results in the form of the ratios of (143) to (141) and (143) to (142), we obtain

$$R_1 = (4\rho/3\pi R)(30\,xd\cos\psi\sin\phi)/[(30 - 45\,x^2)\,x\sin\psi$$

$$+ (4\rho/3\pi R)(150 - 315\,x^2)\,xd\cos\psi\cos\phi], \qquad (144)$$

$$R_2 = (4\rho/3\pi R)(30\,xd\cos\psi\sin\phi)/[(18 - 15\,x^2)\,x\sin\psi$$

$$+ (4\rho/3\pi R)(90 - 105\,x^2)\,xd\cos\psi\cos\phi]. \qquad (145)$$

Using the computed ratios R_1 and R_2, we can solve immediately for ϕ in the form of cot ϕ or tan ϕ, e.g.,

$$\cot\phi = [R_1(10 - 15\,x^2) - R_2(6 - 5\,x^2)]/(8x^2R_1R_2)\,. \qquad (146)$$

In this result x is the known quantity $X_o/R = X_o/(X_o^2 + D^2)^{1/2}$.

This method of determining ϕ from simultaneous measurements at the two surface positions requires that the anomaly signal strength be large enough. It is probable that the one percent ferromagnetic slurry, which leads to signal strengths such as those shown in (132), is marginal. However, the use of a ten percent ferromagnetic slurry would be adequate.

VII. SUMMARY AND CONCLUSIONS

In Sec. II. A. we discuss the well-known formulas used to represent the earth's field at any geographical location and point out that the direction and magnitude of any local paramagnetic moment (Sec. II. B.) polarized by this field will be determined by the earth's field vector. On the other hand, in the case of ferromagnetic particles in slurry (Sec. II. C.), we have had to make the assumption that it is possible to prepare a slurry that will exhibit a large moment aligned parallel to the earth's field vector, after being pumped into the crack produced by hydrofracturing. Unfortunately, unlike the paramagnetic case, there is no guarantee that this assumption will be valid in practice. However, it is reasonable and compelling to believe the validity of this idea. We discuss also in Sec. II. C. some of the factors that must be considered in the selection of a ferromagnetic particle slurry in order that it may have the desired properties.

The equations for the parallel and perpendicular components $\delta B_{||}$ and $\delta B_{\perp}$, respectively, of the static dipole field due to a volume element δv containing polarized magnetic material, are expended into the six cartesian components in (14) to (19). Assuming the magnetic moments m_o of all such volume elements in any chosen volume distribution are uniform, it is then only necessary to integrate these expressions over the distribution to obtain the field at a distance. For convenience, we have chosen to carry out these laborious integrations in spherical coordinates for a spherical distribution in Sec. III. B., for a wedge distribution in Sec. III. C., and for a crack distribution in Sec. III. D. After these integrations were carried out, it was easy to show that the same results could have been obtained, in the first place, by simply differentiating the appropriate scalar magnetic potential function. Unfortunately, there were no guide lines for determining this function in advance, but having determined it from some of the results, it provided a check on the accuracy and consistency of the expressions for B_x, B_y, and B_z.

These resulting expressions, (30)-(32) for the spherical distribution, (40)-(42) for a wedge distribution, and (44)-(46) for a crack distribution, then describe the cartesian components of the overall signal that would be measured by a magnetometer.

Two types of magnetometers are envisioned in this study, e.g., the easy-to-come-by flux gate magnetometer, with sensitivity of the order of 10^{-6} Oe, and the superconducting loop-SQUID magnetometer, with sensitivity as high as 10^{-10} to 10^{-11} Oe. Other types such as the NMR magnetometer, for example, can also be

used and these have sensitivities as high as 10^{-8} 0e. However, no other known magnetometer device has a sensitivity approaching that of the SQUID. The overall signal measured by a magnetometer would include the anomaly contribution plus a combination of earth's field components plus magnetic noise from all sources. Some of the properties of magnetic noise are discussed in Secs. V. A. and V. B.

On the other hand, the sensor of a superconducting gradiometer, such as the SQUID indicated schematically in Fig. 1, would measure a field the value of which is proportional to the appropriate derivatives of (30)-(32), or (40)-(42), or (44)-(46), multiplied by the factor (2S), which is the distance of separation of the two superconducting gradiometer loops. This field is usually 10^{-4} to 10^{-6} times the magnetometer field. Consequently, only the SQUID sensor has high enough sensitivity to be used in conjunction with the superconducting gradiometer configuration, at least for the purposes we consider here. The gradiometer signal also contains the derivatives of the magnetic noise, rather than the noise itself. One of the great advantages of the superconducting gradiometer is that these noise derivatives are often negligibly small.

In addition to the calculations of the fields at arbitrary locations such as (X_o, Y_o, D) on the earth's surface, (14)-(19) can be used to calculate the fields at positions in the borehole. One needs only to replace (X_o, Y_o, D) by $(S\cos\chi, S\sin\chi, d << D)$, which is a position very close to the center of the borehole axis, and then to carry out the indicated integrations over the distribution of magnetic material in the crack. In Sec. IV, to facilitate these integrations, we arbitrarily select a minimum radius r_m for the wedge distribution, and pick d = 0, and obtain the anomaly fields that would be measured by a magnetometer or gradiometer in the borehole.

The mose useful results are for the case of a directional magnetometer, or a gradiometer (which is always directional) with axis in the x-y plane. We consider the cases in which the axes of these borehole devices are rotated in the x-y plane to any arbitrary angle χ, which is measured with respect to magnetic south (x-axis of Fig. 2). The results for the horizontal superconducting axial gradiometer are given by (51)-(56) and these are combined into the actual gradiometer signal in (57). Notice that this final result is a function of both the rotation angle χ of the gradiometer and the orientation angle ϕ of the crack distribution. The directional magnetometer signal given by (58) includes the anomaly contribution as well as the contribution due to the horizontal component of the earth's field [(magnetic noise is excluded from the formula (58)]. The anomaly portions of

these signals are plotted as a function of the angle χ in Figs. 6, 7.

In any practical application to determine the crack orientation, the following procedure would be used: an initial magnetic survey would be made prior to flooding the crack with magnetic material, then later, a final survey would be made after flooding. The latter survey signal would contain the desired anomaly crack information. Unfortunately, there will always be an unavoidable time delay between these initial and final surveys, during which time the diurnal magnetic noise conditions could change by as much as 100 γ. Realization of this difficulty therefore led to the proposal of a new idea in Sec. V. A. for cancelling out the diurnal noise. In this scheme, we would synchronize the rotation of the borehole magnetometer with that of a second magnetometer located at a nearby position on the surface at which the anomaly contribution is negligibly small. Thus, subtraction of these two signals would eliminate all but the random components of the magnetic noise and some small noise gradient contributions. Subtraction would also eliminate the interfering horizontal component of the earth's magnetic field.

We then analyze in (76)-(84) the before and after magnetometer signal differences and find the net difference to be a function of rotation angle χ and crack orientation angle ϕ. A procedure for computerized cross-correlation analysis is outlined in (78)-(84) which should lead to the determination of the desired result, namely the value of the angle ϕ. This procedure should eliminate the interfering magnetic noise contributions that are of a random nature. Unfortunately, this determination of ϕ $\pm$ error carries with it the possibility of an ambiguity of 180°. Thus, the work of Sec. V. A. can be regarded as theoretical demonstration of the feasibility of the proposed scheme for determining ϕ $\pm$ error $\pm$ 180°. It is shown that a ferromagnetic particle slurry must be used in conjunction with the scheme. Unfortunately, the magnetic moment of the crack distribution flooded with a paramagnetic solution gives a signal that is too small for reliable analysis to determine ϕ.

In Sec. V. B. we propose a similar scheme in which now a borehole gradiometer would be rotated in the x-y plane in synchronism with a second nearly identical gradiometer located at an appropriate position on the surface. Again, the two signals would be subtracted and it is shown that this procedure would eliminate the gradient of the earth's field horizontal component and the gradients of the interfering diurnal magnetic noise. Although the procedure calls for an initial (before flooding) and a final (after flooding) survey, the analysis indicates that only a final survey may be necessary.

The results of a complete analysis for a gradiometer rotated in the x-y plane are embodied in (85)-(114). These take into account the effects of noise as well as of gradiometer imperfection. The before flooding and after flooding signal differences should contain essentially the desired anomaly information in the form of the function of (χ,ϕ) as shown in Fig. 7 plus random magnetic noise. We propose a procedure of cross-correlation analysis in which signal plus noise is correlated with three functions. This procedure should lead to the determination of the crack orientation ϕ without ambiguity and with less error than that determined by analysis of magnetometer signals. This superconducting gradiometer scheme is thus found to be the scheme with the greatest degree of theoretical feasibility for determining ϕ. But again, the use of a paramagnetic solution for flooding the crack gives an anomaly that is too small. Again, it is shown that the ferromagnetic particle slurry must be used. However, it is not necessary that the volume of ferromagnetic particles in the slurry be as large as the 1.0 percent figure used in the analysis of borehole anomaly signals.

We derive in Sec. VI. the signals measured by surface magnetometers and gradiometers due to spherical distributions, wedge distributions, and the actual crack distribution. The signal functions that would be produced in axial-type gradiometers by the anomalies due to spherical distributions are tabulated in Table 3 for nine different axis orientations. The importance of these results is that they show how the signal strength can be a function of position on the surface and that one can maximize or minimize the anomaly portion of the signal by proper selection of position. This fact then suggests a scheme in which one gradiometer is placed at the minimum point and a second gradiometer is placed at the maximum point. The two gradiometers would then be rotated in synchronism to the same angle χ and the signals subtracted. This would eliminate the undesirable earth's field-gradient components as well as the gradients due to diurnal noise and leave remaining the function of χ containing the desired anomaly information.

The wedge distribution will produce a signal in a horizontal axial gradiometer located at a position $(X_o, Y_o = 0, D)$ that can be calculated by substituting (125) and (126) into (117). This result is of interest because it shows the part dependent on (χ,ϕ) contains the prefactor (ρ^4/R^4) while the part dependent on (χ) alone is an order of magnitude larger, i.e., the prefactor is (ρ^3/R^3). This means that the amplitude of the (χ,ϕ) portion must be at least an order of magnitude greater than the gradiometer basic sensitivity in order to obtain (χ,ϕ) that can be later analyzed to determine ϕ. In the example shown in (132), the

amplitude of the (χ,ϕ) portion of the signal is not really large enough for later data analysis but two different ways are suggested for increasing this by a factor of 10 to 100.

We calculate in Sec. VI.C. the signals an actual crack anomaly (not its wedge approximation) would produce in vertical and horizontal gradiometers located on the surface. The result in (136) shows that the crack and wedge anomalies produce about the same signal strength which lends support to the various conclusions obtained earlier on the basis of wedge anomaly calculations.

We obtain in (140) the difference between the signal produced in a horizontal axial gradiometer at the point $(X_o,Y_o=0,D)$ and that in a nearly identical gradiometer at $(-X_o,Y_o=0,D)$. This difference, for the fields produced by a crack anomaly at the bottom of the borehole, contains a part which is a function of (χ) with prefactor (ρ^2/R^2) plus a function of (χ,ϕ) with prefactor (ρ^3/R^3). The amplitude of this latter part of the difference signal must be of the order of 10^{-9} Oe or higher in order to process the data defining the angle ϕ. The procedure consists of computer correlations of the difference signal with the function $\cos^2\chi$, $\sin^2\chi$, and $\sin\chi\cos\chi$ over several complete cycles of the angle χ. This procedure eliminates the gradiometer imperfection contributions as well as any magnetic noise that is random. It is indicated in Sec. VI that a crack of 2.0-mm width and radius ρ = 300 m will produce a large enough anomaly if the ferromagnetic particle volume ratio is about 10 percent in the slurry and if a 5-to-1 or 10-to-1 flux transformer scheme is used in conveying the signals from the superconducting gradiometer into the SQUID sensor-shielded housing. Under these conditions the use of surface gradiometers to determine the anomaly orientation angle ϕ is feasible.

To summarize, we have carried out a feasibility study on the question of determining, by magnetic survey methods, the orientation angle ϕ of a crack produced by hydrofracturing in a borehole drilled into a hot rock geothermal source. The method requires flooding a suitable magnetic material into the crack, thereby producing an artificial magnetic anomaly in the earth's field, and then detecting the existence and orientation of the anomaly. It is found that the use of a paramagnetic solution for this purpose will not give a sufficiently large magnetic moment. However, use of prepolarized ferromagnetic particles in a slurry satisfied the requirements for detectability of the anomaly.

A two-superconducting gradiometer scheme, with one in the borehole and the second one on the surface, provides a feasible method of determining ϕ ± smaller

error (without the 180° ambiguity). This is the most feasible system, from the theoretical viewpoint, of all considered in this report. However, the scheme requires a superconducting gradiometer-SQUID system to be housed in a logging device housing that is to be moved into the hot rock zone. The cryogenic engineering technology for such a system is not now in existence and would have to be developed. However, present technology appears capable of this challenge.

Finally, a two-superconducting gradiometer scheme, with one on the surface at at a position (X_o, Y=0, D) and the second one, also on the surface, at ($-X_o$, Y=0, D) provides still another feasible method for determining ϕ ± error (without the 180° ambiguity). However, the error in this scheme will be greater than in the above gradiometer scheme because the ϕ-dependent part of the signal is of smaller amplitude.

All of the above schemes require the use of ferromagnetic particles in slurry in order that the magnetic moment of the crack be sufficiently large. However, the first two schemes can produce a satisfactory determination of ϕ if the particle volume ratio in the slurry is one percent or less. On the other hand, the scheme using only surface gradiometers will require a five to ten percent volume ratio in order to produce a sufficiently large crack magnetic moment.

REFERENCES

1. J. E. Zimmerman, P. Theine, and J. T. Harding, J. Appl. Phys. 41, 1572-1580 (1970).

2. J. E. Mercereau, Rev. Phys. Appl. 5, 13-20 (1970); H. A. Notarys and J. E. Mercereau, Proc. Int. Conf. Science of Superconductivity (Stanford, CA, Aug. 26-29, 1969), F. Chilton, Ed., pp. 424-431.

3. R. P. Giffard, R. A. Webb, and J. C. Wheatley, J. Low Temperature Phys. 6, 533-610 (1972).

4. W. W. Webb, IEEE Trans. Magn., Vol. MAG-8, 51-60 (1972).

5. W. L. Goodman, V. W. Hesterman, L. H. Rorden, and W. S. Goree, Proceedings IEEE 61, No. 1, 20-27, Jan., 1973; J. Clarke, Proceedings IEEE 61, No. 1, 8-19, Jan., 1973.

6. M. Nisenoff, Rev. Phys. Appl. 5, 21-24 (1970); M. Nisenoff, Private communication; F. J. Rachford, C. Y. Huang, M. Nisenoff, and S. A. Wolf, IEEE Transactions on Magnetics, Vol. MAC-11, 870-872, 1975; C. Y. Huang, private communication.

7. T. D. Clark and L. D. Jackel, IEEE Transactions on Magnetics, Vol. MAG-11, 736-738, March, 1975; J. Clarke, W. M. Goubou, and M. B. Ketchen, IEEE Transactions on Magnetics, Vol. MAG-11, 724-726, March, 1975.

8. J. A. Jacobs, Geomagnetic Micropulsations, Springer-Verlag, Berlin(1970); J. A. Jacobs, The Earth's Core and Geomagnetism, (Macmillan Publishing Co., Inc., New York, 1964); S. Matsushita and W.H. Campbell, Physics of Geomagnetic Phenomena,(Academic Press, New York, 1967) and references therein cited.

9. J. E. Mercereau, "Superconducting Magnetometers," Rev. Phys. Appl. 5,13 (1970); W. W. Webb, "Superconducting Quantum Magnetometers," IEEE Trans. Magn. mag 8, 51 (1972); W. M. Wynn, C. P. Frahm, P. J. Carroll, R. H. Clark, J. Wellhoner, and M. J. Wynn, "Advanced Superconducting Gradiometer/Magnetometer Arrays and a Novel Signal Processing Technique," IEEE Trans. Magn. mag 11, 701 (1975).

10. H. A. Notarys, R. H. Wang, and J. E. Mercereau, Proceedings of the IEEE, Vol. 61, 79-84, January, 1973; R. H. Wang, private communication.

11. For example, Develco, Inc., Mountain View, CA 94040; Superconducting Technology, Inc., Mountain View, CA 94040; S. H. E. Corporation, San Diego, CA 92121.

12. J. E. Zimmerman and N. V. Frederick, Appl. Phys. Letters, 19, 16-19 (1971); D. Cohen, IEEE Transactions on Magnetics, Vol. MAG-11, 694-700, March, 1975.

13. For example, U.S. Naval Research Laboratory, Washington, D.C.; Johns Hopkins Applied Physics Laboratory, Silver Spring, MD; Naval Coastal Systems Laboratory, Panama City, FL.

14. The basic idea of producing cracks by hydrofracturing, information as to the expected widths and extents of cracks so produced, and other pertinent information about the geothermal program at LASL has been provided by members of the LASL Q-Division Office and the LASL Geothermal Technology Group.

15. M. Segiura and J. P. Heppner, American Institute of Physics Handbook, D. E. Gray, Coordinating Editor, McGraw Hill Book Company, New York, 1972, pp. 5-264 to 5-273.

16. C. Kittel, Introduction to Solid State Physics, Second Edition, John Wiley and Sons, Inc., New York, 1957.

17. Handbook of Chemistry and Physics, Thirty-Seventh Edition, 1955; Forty-Fifth Edition, The Chemical Rubber Co., Cleveland, OH, 1964.

☆ U.S. GOVERNMENT PRINTING OFFICE: 1976—777-018/35